ELEKTRİK, VOL.1, NO.1, February 1993, ©TÜBİTAK EMO

Two-Dimensional Recursive Autoregressive Lattice Analysis and Synthesis Models For Spectral Estimation

Ahmet H. Kayran
Department of Electrical Engineering
The Technical University of Istanbul
Maslak, Istanbul, Turkey 80626

Abstract

In this paper, autoregressive lattice parameter models for two-dimensional (2-D) spectrum estimation are presented. The theory is based upon the recently developed 2-D lattice modelling technique. It is shown that it is possible to calculate the lattice parameters from only a knowledge of the autocorrelation of the 2-D process. The stability of synthesis model is determined from the lattice parameter factors. Three structurally stable quarter-plane models are given to eliminate the stability test at each stage. Examples are given to illustrate the performance of the proposed method.

1. Introduction

The problem of two-dimensional (2-D) spectral estimation arises in various fields such as seismic signal processing [1], radar [2], sonar [3], image restoration [4], and radio astronomy. Consequently, it has been subject to intensive research over the past several years.

An excellent up to date review of multidimensional spectral estimation has been made by McClellan [5]. In this paper, seven different classes of spectral estimation methods have been discussed. It was shown that five of these classes are exactly parallel to the one-dimensional (1-D) situation. Namely, these are the classical methods based on the discrete Fourier transform, the maximum likelihood method [6], the autoregressive (AR) method, the maximum entropy method due to Burg [7], and a generalization of the Pisarenko's method [8]. The other two classes have no exact counterparts in 1-D Spectral estimation. One is the class of separable estimators [9], where 1-D estimator is employed along each of the individual dimensions. The other method is based upon the data extensions for spectral estimation. In this case, the extension can be made by linear prediction [10], or band-limited extrapolation [11].

Several AR models are proposed for the 2-D spectral estimation in the literature [12]-[19]. It is known that the primary issue with the 2-D AR modelling is the choice of the prediction error mask and the order of computation for the recursive model. Jackson and Chien [12] have discussed the different quadrant AR models to obtain an estimator that is more nearly circularly symmetric. Kumaresan and Tufts [13] have described a similar method for a simultaneous frequency and wavenumber estimation. The order of this model [13] is the highest allowable, i.e., an $M \times N$ prediction error filter for $M \times N$ array of data.

Jain and Ranganath [14] suggest the use of semicasual and noncausal models. For the semicausal case the prediction error mask includes samples in the past of one direction but uses the past and future in the other direction. It is shown that this estimate is not strictly all-pole; a numerator term is also generated. Woods [15],

Newman [16], Cadzow and Ogino [17], and Tjostheim [18] have also proposed using AR modelling to obtain a spectral estimate.

However, all of these AR models [12]-[19] have been developed without use of 2-D lattice parameters. The first fundamental approach to the use of the reflection coefficient approach to the modelling of 2-D fields was made by Marzetta [20]-[21] who developed a class of 2-D minimum-phase digital filters involving a sequence of parameters called reflection coefficients. This method was successfully applied to the design of 2-D recursive filters [22] and linear predictive coding of images [23].

In this paper, a new AR technique is developed for estimating the spectral characteristic of a 2-D random field from its autocorrelation function. The theory is based upon the recently presented AR lattice modelling of 2-D fields [25], [27]. The results outlined in the succeeding sections can be applied to any 2-D autocorrelation function of given dynamic 2-D systems. The proposed method estimates the 2-D spectrum stage by stage and does not require a priori order determination. The determination of the stability of 2-D lattice AR models is made using 2-D lattice parameters computed at each stage, as in the 1-D case.

In Section 2, 1-D lattice parameter theory is briefly reviewed. It is shown how to calculate the lattice parameter factors from the given autocorrelation function. Moreover, the forward, backward and Burg's methods are unified in a matrix form of the prediction error sequences. The quarter-plane AR lattice parameter theory is developed as a natural extension of the 1-D lattice theory in Section 3. Starting with a given autocorrelation function, three lattice parameter factors are obtained at each stage. Lattice coefficients are then used to generate four prediction error filters for successive lattice parameter model stages. The technique does not involve modifying the correlation function, and updates the prediction error filter coefficients. Lattice parameters are computed by minimizing the mean-square value of the prediction error fields as defined. In Section 4, quarter-plane AR modelling is extended to the asymmetric half-plane. Two asymmetric half-plane models are discussed with different recursion directions. The algorithms indicate how the appropriate asymmetric half-plane parameters are calculated from a given autocorrelation function. Synthesis model conditions for lattice model stability are described in Section 5. In Section 6, structurally stable quarter-plane lattice models are discussed. Finally, in Section 7, several numerical examples are given to support the theory.

2. One-Dimensional Autoregressive Lattice Modelling Using the Correlation Values

Lattice parameter modelling of one-dimensional stationary signals is based upon the following equation:

$$\mathbf{e}^{(n+1)}(k) = \mathbf{K}^{(n+1)}\mathbf{e}^{(n)}(k)^* \tag{1a}$$

where

$$e^{(n)}(k) = [e_f^{(n)}(k)e_b^{(n)}(k)]^T \tag{1b}$$

$$e^{(n)}(k)^* = [e_f^{(n)}(k)e_b^{(n)}(k-1)]^T \tag{1c}$$

and

$$\mathbf{K}^{(n)} = \begin{bmatrix} 1 & -k^{(n)} \\ -k^{(n)} & 1 \end{bmatrix} \tag{1d}$$

The forward and backward prediction error sequences, $e_f^{(n+1)}(k)$ and $e_b^{(n+1)}(k)$ respectively, for the $(n+1)$-th order lattice model stage are calculated from the error sequences of the (n)-th order lattice model stage.

The lattice parameter factor $k^{(n+1)}$ is calculated using the output prediction error sequences of the previous stage. Thus starting from $n = 0$ with $e_f^{(0)}(k) = e_b^{(0)}(k) = y(k)$, where $y(k)$ is a given input sequence, it is possible to calculate forward and backward prediction error sequences from (1a) for successively higher order lattice models. The lattice parameter reflection factor can be computed by minimizing the mean squared value of the prediction error sequences. The following mean squared error is defined by the $(n+1)$-th order lattice model

$$Q^{(n+1)} = E[\mathbf{e}^{(n+1)^T}(k)\mathbf{\Lambda}_D\mathbf{e}^{(n+1)}(k)] \tag{2}$$

where $E[\cdot]$ denotes the expected value over a block of data. In (2) $\mathbf{\Lambda}_D = \text{diag.matrix}[\lambda_1\ \lambda_2]$. The λ_1 and λ_2 are arbitrary weights, taken to be either 0 or 1, to be associated with the expected values of the forward and backward prediction error sequences, e_f, e_b respectively.

The results of this minimization are summarized by the following equation.

$$k^{(n+1)} = \frac{E[\mathbf{e}^{(n)^T}(k)^*\tilde{\mathbf{I}}\mathbf{\Lambda}_D\mathbf{e}^{(n)}(k)^*]}{E[\mathbf{e}^{(n)^T}(k)^*\tilde{\mathbf{I}}\mathbf{\Lambda}_D\tilde{\mathbf{I}}\mathbf{e}^{(n)}(k)^*]} \tag{3}$$

where $\tilde{\mathbf{I}}$ is the anti-diagonal unity matrix and will be discussed in the next section.

The following methods are widely used for the computation of $k^{(n+1)}$ in the literature [7], [24].

a) Forward Method $(\lambda_1 = 1, \lambda_2 = 0)$*;*

$$k_f^{(n+1)} = \frac{E[e_f^{(n)}(k)e_b^{(n)}(k-1)]}{E[e_b^{(n)^2}(k-1)]} \tag{4a}$$

b) Backward Method $(\lambda_1 = 0, \lambda_2 = 1)$*;*

$$k_b^{(n+1)} = \frac{E[e_f^{(n)}(k)e_b^{(n)}(k-1)]}{E[e_f^{(n)^2}(k)]} \tag{4b}$$

c) Burg's Method $(\lambda_1 = \lambda_2 = 1)$*;*

$$k_{\text{BURG}}^{(n+1)} = \frac{2E[e_f^{(n)}(k)e_b^{(n)}(k-1)]}{E[e_f^{(n)^2}(k)] + E[e_b^{(n)^2}(k-1)]} \tag{4c}$$

Since the quantities $e_f^{(n)}(k)$ and $e_b^{(n)}(n)$ are sums of weighted present and past values of the input $y(k)$, the numerator and denominator of (4a)-(4c) can be expressed as the weighted sum of correlations of the input vector $\mathbf{Y}$. An algorithm based upon this observation can be expected to be computationally efficient, if the correlations of the input signal are known since it is not necessary to update the error sequences at each lattice stage.

It is possible to write the forward error signal as

$$e_f^{(n)}(k) = \mathbf{Y}^{(n)^T}(k)\mathbf{W}^{(n)} \tag{5a}$$

where

$$\mathbf{Y}^{(n)}(k) = [y(k), y(k-1) \cdots y(k-n)]^T \tag{5b}$$

$$\mathbf{W}^{(n)} = \left[w_0^{(n)} w_1^{(n)} \cdots w_n^{(n)}\right]^T \tag{5c}$$

Similarly, $e_b^{(n)}(k)$ can be written

$$e_b^{(n)}(k) = \mathbf{Y}^{(n)^T} \tilde{\mathbf{I}} \mathbf{W}^{(n)} \tag{6}$$

where $\tilde{\mathbf{I}}$ is extended to the appropriate order. From (5) and (6),

$$e_b^{(n)}(k-1) = \mathbf{Y}^{(n+1)^T} \tilde{\mathbf{I}} \hat{\mathbf{W}}^n \tag{7a}$$

where

$$\hat{\mathbf{W}}^{(n)} = \left[\mathbf{W}^{(n)^T} : 0\right]^T \tag{7b}$$

Substituting (5a) and (7a), into (1a) yields

$$\begin{bmatrix} e_f^{(n+1)}(k) \\ e_b^{(n+1)}(k) \end{bmatrix} = \left[\begin{array}{c|c} \mathbf{Y}^{(n+1)^T} & \mathbf{O}^T \\ \cdots & \cdots \\ \mathbf{O}^T & \mathbf{Y}^{(n+1)^T} \end{array}\right] \begin{bmatrix} \mathbf{W}^{(n+1)} \\ \cdots \\ \tilde{\mathbf{I}}\mathbf{W}^{(n+1)} \end{bmatrix} \tag{8a}$$

where

$$\mathbf{W}^{(n+1)} = \hat{\mathbf{W}}^{(n)} - \mathbf{k}^{(n+1)} \tilde{\mathbf{I}} \hat{\mathbf{W}}^{(n)} \tag{8b}$$

It should be noted that the initial condition for the weighted factor $\mathbf{W}^{(0)}$ is

$$\mathbf{W}^{(0)} = [1] \tag{8c}$$

The numerators of equations (4a)-(4c) can now be rewritten using the definition of the error signals in terms of the weight vectors

$$\begin{aligned} E[e_f^{(n)}(k) e_b^{(n)}(k-1)] &= E[\hat{\mathbf{W}}^{(n)^T} \mathbf{Y}^{(n+1)} \mathbf{Y}^{(n+1)^T} \tilde{\mathbf{I}} \hat{\mathbf{W}}^{(n)}] \\ &= \hat{\mathbf{W}}^{(n)} \mathbf{R}^{(n+1)} \tilde{\mathbf{I}} \hat{\mathbf{W}}^{(n)} \end{aligned} \tag{9}$$

where $\mathbf{R}^{(n)}$ is the correlation matrix of the input signal.

$$\mathbf{R}^{(n)} = \begin{bmatrix} r_{yy}(0) & r_{yy}(1) & \cdots & r_{yy}(n) \\ r_{yy}(-1) & r_{yy}(0) & & \vdots \\ \vdots & & & r_{yy}(1) \\ r_{yy}(-n) & \cdots & r_{yy}(-1) & r_{yy}(0) \end{bmatrix} \tag{10}$$

Since the correlation matrix in (10) is symmetric and toeplitz, (9) can be written as summations:

$$\begin{aligned} E[e_f^{(n)}(k) e_b^{(n)}(k-1)] &= r_{yy}(0) \sum_{i=0}^{n} w_i^{(n)} w_{n-i+1}^{(n)} \\ &+ r_{yy}(1) \left[\sum_{i=0}^{n} w_i^{(n)} w_{n-i}^{(n)} + \sum_{i=2}^{n} w_i^{(n)} w_{n-i+2}^{(n)}\right] \\ &+ r_{yy}(2) \left[\sum_{i=0}^{n} w_i^{(n)} w_{n-i-1}^{(n)} + \sum_{i=3}^{n} w_i^{(n)} w_{n-i+3}^{(n)}\right] \\ &+ \cdots + r_{yy}(n+1) w_0^{(n)^2} \end{aligned} \tag{11}$$

The denominators of equations (4a)-(4c) can be found by using similar arguments. However, the following recursion is generally used;

$$Q^{(0)} = r_{yy}(0) \tag{12a}$$

$$Q^{(n)} = Q^{(n-1)}\left(1 - k^{(n)^2}\right) \tag{12b}$$

Equation (12) is used to compute the denominator term in (4) to calculate the lattice parameter reflection factor $k^{(n+1)}$.

3. Quarter-Plane Autoregressive Lattice Modelling

The basic theory of the quarter-plane AR lattice parameter modelling for a given stationary random data field has recently been developed in [25]. The prediction error fields, corresponding to the forward and backward prediction error sequences in the 1-D case [24], are defined by the following equation:

$$\mathbf{e}_{QP}^{(\mathbf{n+1})}(k_1, k_2) = \mathbf{K}_{QP}^{(\mathbf{n+1})}\mathbf{e}_{QP}^{(\mathbf{n})}(k_1, k_2)^* \tag{13a}$$

where $(\mathbf{n}) = (n_1, n_2)$ is the order of the model and $(\mathbf{n+1}) = (n_1 + 1, n_2 + 1)$. The error fields are defined by

$$\mathbf{e}_{QP}^{(\mathbf{n})}(k_1, k_2) = \left[e_{0,0}^{(\mathbf{n})}(k_1, k_2)e_{1,0}^{(\mathbf{n})}(k_1, k_2)e_{1,1}^{(\mathbf{n})}(k_1, k_2)e_{0,1}^{(\mathbf{n})}(k_1, k_2)\right]^T \tag{13b}$$

$$\mathbf{e}_{QP}^{(\mathbf{n})}(k_1, k_2) = \Big[e_{0,0}^{(\mathbf{n})}(k_1, k_2)e_{1,0}^{(\mathbf{n})}(k_1 - 1, k_2) \\ e_{1,1}^{(\mathbf{n})}(k_1 - 1, k_2 - 1)e_{0,1}^{(\mathbf{n})}(k_1, k_2 - 1)\Big]^T \tag{13c}$$

and

$$\mathbf{K}_{QP}^{(\mathbf{n})} = \begin{bmatrix} 1 & -k_{1,0}^{(\mathbf{n})} & -k_{1,1}^{(\mathbf{n})} & -k_{0,1}^{(\mathbf{n})} \\ -k_{1,0}^{(\mathbf{n})} & 1 & -k_{0,1}^{(\mathbf{n})} & -k_{1,1}^{(\mathbf{n})} \\ -k_{1,1}^{(\mathbf{n})} & -k_{0,1}^{(\mathbf{n})} & 1 & -k_{1,0}^{(\mathbf{n})} \\ -k_{0,1}^{(\mathbf{n})} & -k_{1,1}^{(\mathbf{n})} & -k_{1,0}^{(\mathbf{n})} & 1 \end{bmatrix} \tag{13d}$$

$\mathbf{K}_{QP}^{(\mathbf{n})}$ can be written in a more compact form as

$$\mathbf{K}_{QP}^{(\mathbf{n})} = \mathbf{I} - k_{1,0}^{(\mathbf{n})}\mathbf{P} - k_{1,1}^{(\mathbf{n})}\tilde{\mathbf{P}} - k_{0,1}^{(\mathbf{n})}\tilde{\mathbf{I}} \tag{13e}$$

where $\mathbf{I}$ is the unity matrix and $\mathbf{P}, \tilde{\mathbf{I}}, \tilde{\mathbf{P}}$ are permutation matrices defined

$$\tilde{\mathbf{I}} = \begin{bmatrix} 0 & 0 & 0 & 1 \\ 0 & 0 & 1 & 0 \\ 0 & 1 & 0 & 0 \\ 1 & 0 & 0 & 0 \end{bmatrix}; \mathbf{P} = \begin{bmatrix} 0 & 1 & 0 & 0 \\ 1 & 0 & 0 & 0 \\ 0 & 0 & 0 & 1 \\ 0 & 0 & 1 & 0 \end{bmatrix}; \tilde{\mathbf{P}} = \begin{bmatrix} 0 & 0 & 1 & 0 \\ 0 & 0 & 0 & 1 \\ 1 & 0 & 0 & 0 \\ 0 & 1 & 0 & 0 \end{bmatrix} \tag{13f}$$

$$e_{i,j}^{(n)}(k_1, k_2), (i, j) \in D_{QP}; D_{QP} = \{(0,0), (1,0), (1,1), (0,1)\}$$

are defined as the quarter-plane prediction error fields for the $(\mathbf{n})$-order lattice model. $k_{1,0}^{(\mathbf{n})}, k_{1,1}^{(\mathbf{n})}$ and $k_{0,1}^{(\mathbf{n})}$ are the 2-D lattice parameter reflection factors. Assuming that they are known, and starting from the zero order

model $(\mathbf{n}) = (\mathbf{0})$, with $e_{i,j}^{(\mathbf{0})}(k_1, k_2) = y(k_1, k_2), (i,j) \in D_{QP}$, the inital random field generates four prediction error fields; namely $e_{i,j}^{(\mathbf{i})}(k_1, k_2)$, where $(i,j) \in D_{QP}$. The data of these four fields; are then combined linearly to calculate the prediction error fields of successively higher order stages. The generation of the prediction error fields is depicted in Fig. 1. In generating the prediction error fields of the $(\mathbf{n}+\mathbf{1})$-th order model, the terms of each of the four prediction error fields of the $(\mathbf{n})$-th order model are weighted and combined linearly in four different ways. In Fig. 1 the error field term in the small square is weighted by unity, whereas the other three terms are weighted by $k_{1,0}^{(\mathbf{n+1})}, k_{1,1}^{(\mathbf{n+1})}$ and $k_{0,1}^{(\mathbf{n+1})}$ respectively.

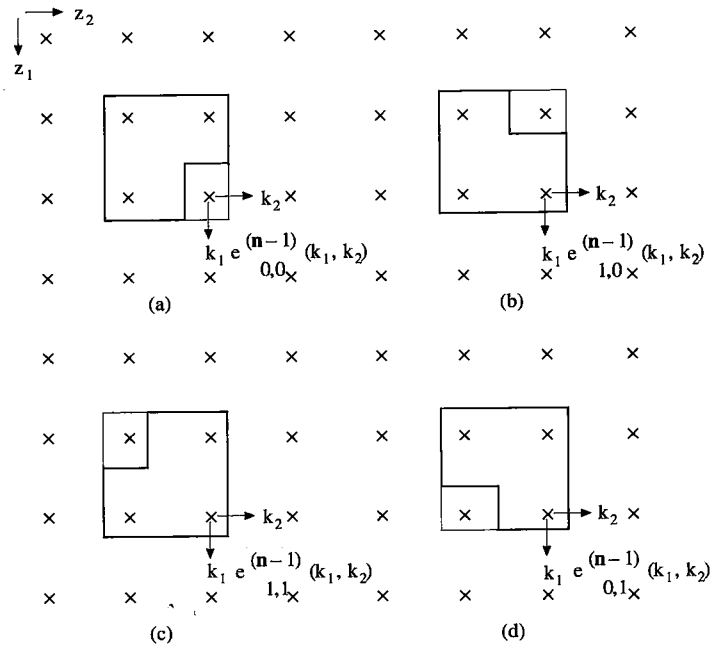

Figure 1. The quarter-plane error fields of order $(\mathbf{n}-\mathbf{1})$ used to generate prediction error fields of order $(\mathbf{n})$

Starting with four data points in the upper left hand corner of each of the four prediction error fields $e_{i,j}^{(\mathbf{n-1})}(k_1, k_2), (i,j) \in D_{QP}$, the data is processed as indicated in Fig. 2 to calculate the four prediction error fields of the next higher $(\mathbf{n})$-th order lattice model. The reflection factor matrix, $\mathbf{K}_{QP}^{(\mathbf{n})}$ is assumed to be symmetric, indicating that the weights applied along the same column, the same row, and the same major diagonal are respectively invariant. The assumption of quarter-plane data propagation is not particularly restrictive and leads to a quarter-plane AR model.

In order to calculate the lattice parameter reflection factors at each stage, the expected mean-squared value of the prediction error fields is minimized with respect to the reflection factors. The following mean-squared error is defined by the $(\mathbf{n}+\mathbf{1})$-order lattice model.

$$Q_{QP}^{(\mathbf{n+1})} = E[e_{QP}^{(\mathbf{n+1})^T}(k_1, k_2)\mathbf{\Lambda}_{QP} e_{QP}^{(\mathbf{n+1})}(k_1, k_2)] \tag{14}$$

where $E[\cdot]$ denotes the expected value over the field of dimension $(K_1 - n_1)(K_2 - n_2)$. In (14), $\mathbf{\Lambda}_{DQ} =$ diag.matrix$[\lambda_1\ \lambda_2\ \lambda_3\ \lambda_4]$. The $\lambda_1, \lambda_2, \lambda_3, \lambda_4$ are arbitrary weights, taken to be either 0 or 1, to be associated with the expected values of the four prediction error fields; $e_{0,0}, e_{1,0}, e_{1,1}$ and $e_{0,1}$ respectively. Substituting

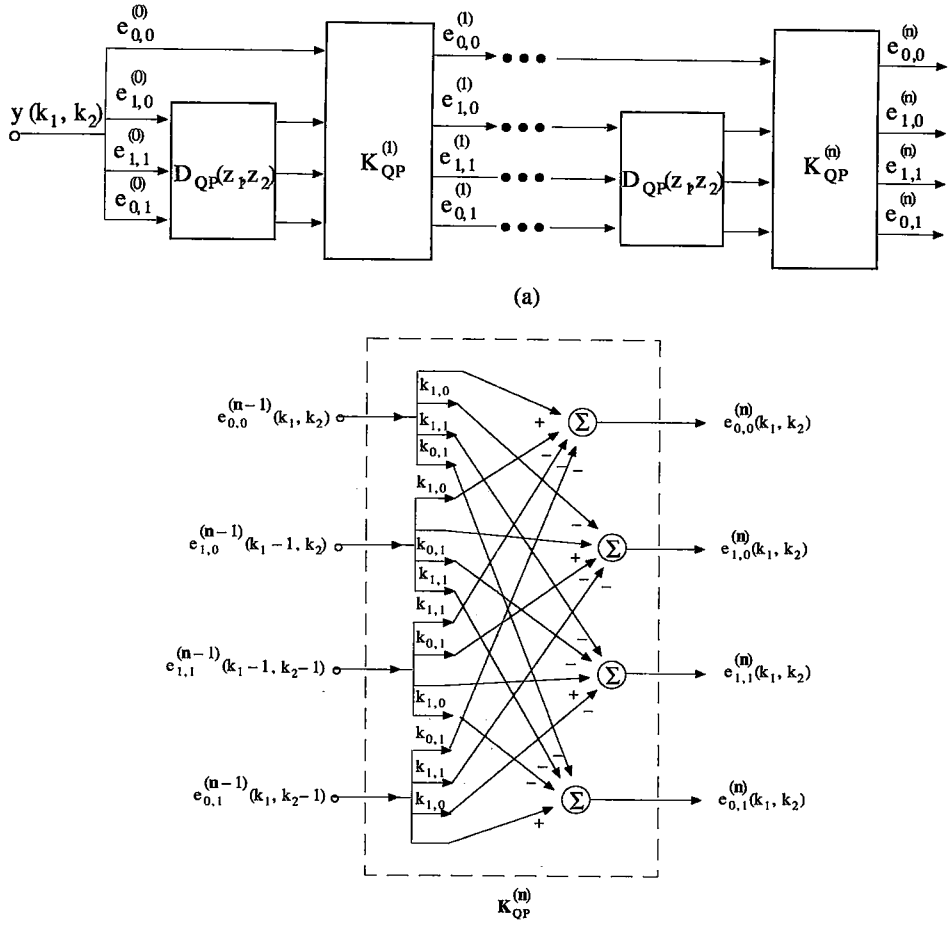

Figure 2. Generation of 2-D quarter-plane prediction error fields (analysis model); (a) internal block structure, (b) block interconnection.

(13a) into (14) results in an expression which can be minimized with respect to lattice model reflection factors. The results of this minimization are summarized in the following equation.

$$\mathbf{R}_{QP}^{(\mathbf{n})}\mathbf{k}_{QP}^{(\mathbf{n+1})} = \mathbf{r}_{QP}^{(\mathbf{n})} \tag{15a}$$

where

$$\mathbf{R}_{QP}^{(\mathbf{n})} = \left[R_{pq}^{(\mathbf{n})}\right]_{p,q=1}^{3,3} \tag{15b}$$

$$\mathbf{k}_{QP}^{(\mathbf{n})} = \left[k_{1,0}^{(\mathbf{n})}\ k_{1,1}^{(\mathbf{n})}\ k_{0,1}^{(\mathbf{n})}\right]^T \tag{15c}$$

and

$$\mathbf{r}_{QP}^{(\mathbf{n})} = \left[r_{i1}^{(\mathbf{n})}\right]_{i=1}^{3} \tag{15d}$$

$(\mathbf{n}+\mathbf{1})$-th order new prediction error is found by substituting (13a) into (14). Simplifying the result yields

$$Q_{QP}^{(\mathbf{n+1})} = Q_{QP}^{(\mathbf{n})} - \frac{1}{2}k_{QP}^{(\mathbf{n+1})^T}\mathbf{R}_{QP}^{(\mathbf{n})}\mathbf{k}_{QP}^{(\mathbf{n+1})} \tag{15e}$$

If the error correlation matrix $\mathbf{R}_{QP}^{(\mathbf{n})}$ is positive definite, the minimum mean square prediction error will decrease with successive stages.

The terms of the symmetric $\mathbf{R}_{QP}^{(\mathbf{n})}$ matrix and $\mathbf{r}_{QP}^{(\mathbf{n})}$ are defined in Table 1 for values of $\lambda_1, \lambda_2, \lambda_3, \lambda_4$ equal to unity corresponding to the minimization of expected value of the prediction error fields respectively. In Table 1, the term, $\psi_{QP}^{(\mathbf{n})}$ is the error correlation matrix,

$$\psi_{QP}^{(\mathbf{n})} = E[\mathbf{e}_{QP}^{(\mathbf{n})}(k_1, k_2)^* \mathbf{e}_{QP}^{(\mathbf{n})^T}(k_1, k_2)^*] \tag{16}$$

Table 1. Prediction Error Covariances for the Quarter-Plane Model [1]

$R_{11}^{(\mathbf{n})}$	$\psi_{QP}^{(\mathbf{n})} o[2\mathbf{P}\mathbf{\Lambda}_{DQ}\tilde{P}]$
$R_{12}^{(\mathbf{n})}$	$\psi_{QP}^{(\mathbf{n})} o[\mathbf{P}\mathbf{\Lambda}_{DQ}\tilde{\mathbf{I}} + \tilde{\mathbf{I}}\mathbf{\Lambda}_{DQ}\mathbf{P}]$
$R_{13}^{(\mathbf{n})}$	$\psi_{QP}^{(\mathbf{n})} o[\mathbf{P}\mathbf{\Lambda}_{DQ}\tilde{\mathbf{P}} + \tilde{\mathbf{P}}\mathbf{\Lambda}_{DQ}\mathbf{P}]$
$R_{22}^{(\mathbf{n})}$	$\psi_{QP}^{(\mathbf{n})} o[2\mathbf{I}\mathbf{\Lambda}_{DQ}\tilde{\mathbf{I}}]$
$R_{23}^{(\mathbf{n})}$	$\psi_{QP}^{(\mathbf{n})} o[\tilde{\mathbf{I}}\mathbf{\Lambda}_{DQ}\tilde{\mathbf{P}} + \tilde{\mathbf{P}}\mathbf{\Lambda}_{DQ}\tilde{\mathbf{I}}]$
$R_{33}^{(\mathbf{n})}$	$\psi_{QP}^{(\mathbf{n})} o[2\tilde{\mathbf{P}}\mathbf{\Lambda}_{DQ}\tilde{\mathbf{P}}]$
$r_{11}^{(\mathbf{n})}$	$\psi_{QP}^{(\mathbf{n})} o[\mathbf{P}\mathbf{\Lambda}_{DQ} + \mathbf{\Lambda}_{DQ}\mathbf{P}]$
$r_{21}^{(\mathbf{n})}$	$\psi_{QP}^{(\mathbf{n})} o[\tilde{\mathbf{I}}\mathbf{\Lambda}_{DQ} + \mathbf{\Lambda}_{DQ}\tilde{\mathbf{I}}]$
$r_{31}^{(\mathbf{n})}$	$\psi_{QP}^{(\mathbf{n})} o[\tilde{\mathbf{P}}\mathbf{\Lambda}_{DQ} + \mathbf{\Lambda}_{DQ}\tilde{\mathbf{P}}]$

From Fig.2, it is possible to express all the shifted error fields in $e_{QP}^{(\mathbf{n})}(k_1, k_2)^*$ in terms of sums of weighted present and past values of data field. A 2-D stationary random data field is given by the following matrix where $k_1 = 1, 2, \ldots, K_1, k_2 = 1, 2, \ldots, K_2$.

$$\mathbf{Y}(k_1, k_2) = \begin{bmatrix} y(1,1) & y(1,2) & \cdots & y(1,K_2) \\ y(2,1) & y(2,2) & \cdots & y(2,K_2) \\ \vdots & & & \vdots \\ y(K_1,1) & y(K_1,2) & \cdots & y(K_1,K_2) \end{bmatrix} \tag{17}$$

An algorithm based upon this observation can be expected to be computationally more efficient than the previous algorithm in [25]. If the correlation matrix of the data in (17) is known it is not necessary to update four prediction error fields $e_{0,0}, e_{1,0}, e_{1,1}$, and $e_{0,1}$ at each stage. It will be shown that updating the coefficients of the prediction error filters is sufficient to compute the lattice parameter factors.

A. Calculation of Lattice Parameters from the Autocorrelation Function

From the 2-D lattice analysis model in Fig. 2, the prediction error fields can be written as

$$e_{i,j}^{(\mathbf{n})}(k_1, k_2) = \mathbf{Y}_{QP}^{(\mathbf{n})^T} \mathbf{W}_{b_{i,j}}^{(\mathbf{n})}, \quad (i,j) \in D_{QP} \tag{18a}$$

where

$$\mathbf{Y}_{QP}^{(\mathbf{n})} = [\mathbf{y}_{QP}^{(\mathbf{n})^T}(0) \vdots \cdots \vdots \mathbf{y}_{QP}^{(\mathbf{n})^T}(n_i)]^T \tag{18b}$$

$$\mathbf{W}_{b_{i,j}}^{(\mathbf{n})} = [\mathbf{b}_{i,j}^{(\mathbf{n})^T}(0) \vdots \cdots \vdots \mathbf{b}_{i,j}^{(\mathbf{n})^T}(n_i)]^T \tag{18c}$$

[1] $[a_{ij}]o[b_{ij}] := \sum_j \sum_i a_{ij} b_{ij}$

with

$$\mathbf{y}_{QP}^{(\mathbf{n})}(p) = [y(k_1 - p, k_2) \cdots y(k_1 - p, k_2 - n_2)] \tag{18d}$$

$$\mathbf{b}_{i,j}^{(\mathbf{n})}(p) = [b_{i,j}^{(\mathbf{n})}(p, 0) \cdots b_{i,j}^{(\mathbf{n})}(p, n_2)] \tag{18e}$$

$$p = 0, 1, \ldots, n_1$$

where

$$\left[b_{i,j}^{(\mathbf{n})}(p, q)\right]_{p,q=0}^{n_1,n_2}, \quad (i, j) \in D_{QP}$$

is the coefficient matrix of the prediction error transfer function, $B_{i,j}^{(\mathbf{n})}(z_1, z_2)$ which is defined as

$$B_{i,j}^{(\mathbf{n})}(z_1, z_2) = \frac{E_{i,j}^{(\mathbf{n})}(z_1, z_2)}{Y(z_1, z_2)} \tag{19a}$$

with

$$E_{i,j}^{(\mathbf{n})}(z_1, z_2) = Z[e_{i,j}^{(\mathbf{n})}(k_1, k_2)] \tag{19b}$$

$$Y(z_1, z_2) = Z[\mathbf{Y}(k_1, k_2)] \tag{19c}$$

where $Z[\cdot]$ denotes the 2-D z-transform.

The formulation of this algorithm (2-D extension of Levinson's algorithm) is given in reference [25]. Hence it will not be repeated in this paper. From (13a) and (19a), it can be shown [25] that

$$B_{1,0}^{(\mathbf{n})} = \tilde{\mathbf{I}}\mathbf{B}_{0,0}^{(\mathbf{n})} \tag{20a}$$

$$B_{1,1}^{(\mathbf{n})} = \tilde{\mathbf{I}}\mathbf{B}_{0,0}^{(\mathbf{n})}\tilde{\mathbf{I}} \tag{20b}$$

$$B_{0,1}^{(\mathbf{n})} = \mathbf{B}_{0,0}^{(\mathbf{n})}\tilde{\mathbf{I}} \tag{20c}$$

with

$$\mathbf{B}_{i,j}^{(\mathbf{n})} \triangleq \left[b_{i,j}^{(\mathbf{n})}(p, q)\right]_{p,q=0}^{n_1,n_2} \tag{20d}$$

where $\tilde{\mathbf{I}}$ is given by (13e) extended to the appropriate order. Fig.3 shows the support of the filter coefficients for the quarter-plane.

Substituting (20) into (18a) yields

$$\mathbf{e}_{i,j}^{(\mathbf{n})}(k_1, k_2) = \mathbf{Y}_{QP}^{(\mathbf{n})T}\mathbf{I}_{i,j}\mathbf{W}_{b_{0,0}}^{(\mathbf{n})}, \quad (i, j) \in D_{QP} \tag{21a}$$

where $\mathbf{I}_{0,0}$ is the unity matrix. $\mathbf{I}_{1,0}, \mathbf{I}_{1,1}$, and $\mathbf{I}_{0,1}$ matrices are defined in an appropriate order as

$$\mathbf{I}_{1,0} = \begin{bmatrix} \mathbf{O} & & \mathbf{I} \\ & \mathbf{I} & \\ \mathbf{I} & & \mathbf{O} \end{bmatrix}; \mathbf{I}_{1,1} = \begin{bmatrix} \mathbf{O} & & \tilde{\mathbf{I}} \\ & \tilde{\mathbf{I}} & \\ \tilde{\mathbf{I}} & & \mathbf{O} \end{bmatrix}; \mathbf{I}_{0,1} = \begin{bmatrix} \tilde{\mathbf{I}} & & \mathbf{O} \\ & \tilde{\mathbf{I}} & \\ \mathbf{O} & & \tilde{\mathbf{I}} \end{bmatrix} \tag{21b}$$

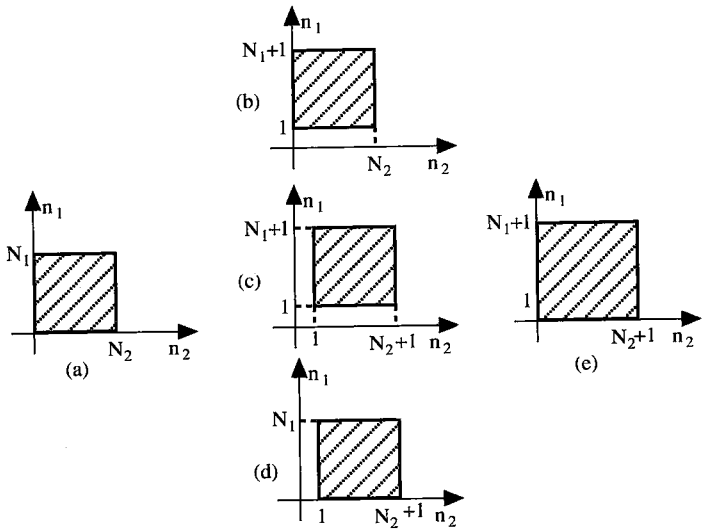

Figure 3. Geometry of the recursion for the quarter-plane model.

It is necessary to obtain the shifted prediction error vector, $e_{QP}^{(\mathbf{n})}(k_1,k_2)^*$ for the computation of the error covariance matrix $\psi_{QP}^{(\mathbf{n})}$, in (16). From (21a), $e_{QP}^{(\mathbf{n})}(k_1,k_2)^*$ can be written as

$$\mathbf{e}_{QP}^{(\mathbf{n})}(k_1,k_2)^* = \hat{\mathbf{Y}}^{(\mathbf{n+1})}\hat{\mathbf{I}}\hat{\mathbf{W}}_{0,0}^{(\mathbf{n})} \tag{22a}$$

where

$$\hat{\mathbf{Y}}^{(\mathbf{n})} = \text{block diag.}[\mathbf{Y}_{QP}^{(\mathbf{n})^T} \vdots \mathbf{Y}_{QP}^{(\mathbf{n})^T} \vdots \mathbf{Y}_{QP}^{(\mathbf{n})^T} \vdots \mathbf{Y}_{QP}^{(\mathbf{n})^T}] \tag{22b}$$

$$\hat{\mathbf{I}} = \text{block diag.}[\mathbf{I}_{0,0} \vdots \mathbf{I}_{1,0} \vdots \mathbf{I}_{1,1} \vdots \mathbf{I}_{0,1}]^T \tag{22c}$$

and $\hat{\mathbf{W}}_{b_{0,0}}^{(\mathbf{n})}$ is the augmented version of $\mathbf{W}_{b_{0,0}}^{(\mathbf{n})}$ defined by

$$\hat{\mathbf{W}}_{b_{0,0}}^{(\mathbf{n})} = [\hat{\mathbf{b}}_{0,0}^{(\mathbf{n})^T}(0) \vdots \cdots \vdots \hat{\mathbf{b}}_{0,0}^{(\mathbf{n})^T}(n_1) \vdots \mathbf{O}^T]^T \tag{22d}$$

with

$$\hat{\mathbf{b}}_{0,0}^{(\mathbf{n})}(p) = [b_{0,0}^{(\mathbf{n})}(p,0) \cdots b_{0,0}^{(\mathbf{n})}(p,n_2)0]^T \tag{22e}$$

$$p = 0,1,\ldots,n_1$$

substitution of (22a) into (16) yields

$$\psi_{QP}^{(\mathbf{n})} = E[\widehat{\widehat{\mathbf{W}}}_{b_{0,0}}^{(\mathbf{n})^T} \hat{\mathbf{I}}^T \hat{\mathbf{Y}}_{QP}^{(\mathbf{n+1})} \hat{\mathbf{Y}}_{QP}^{(\mathbf{n+1})^T} \hat{\mathbf{I}} \widehat{\widehat{\mathbf{W}}}_{b_{0,0}}^{(\mathbf{n})}] \tag{23a}$$

where

$$\widehat{\widehat{\mathbf{W}}}_{b_{0,0}}^{(\mathbf{n})} = \left[\widehat{\mathbf{W}}_{b_{0,0}}^{(\mathbf{n})} \vdots \widehat{\mathbf{W}}_{b_{0,0}}^{(\mathbf{n})} \vdots \widehat{\mathbf{W}}_{b_{0,0}}^{(\mathbf{n})} \vdots \widehat{\mathbf{W}}_{b_{0,0}}^{(\mathbf{n})}\right]^T \tag{23b}$$

Define

$$\hat{\mathbf{R}}_{yy}^{(\mathbf{n})} = E[\mathbf{Y}_{QP}^{(\mathbf{n})} \mathbf{Y}_{QP}^{(\mathbf{n})^T}] \tag{24}$$

Thus (23) can be rewritten as

$$\psi_{QP}^{(\mathbf{n})} = \widehat{\widetilde{\mathbf{W}}}_{b_{0,0}}^{(\mathbf{n})^T} \hat{\mathbf{I}}^T \hat{\mathbf{R}}_{yy}^{(\mathbf{n+1})} \hat{\mathbf{I}} \widehat{\widetilde{\mathbf{W}}}_{b_{0,0}}^{(\mathbf{n})} \tag{25}$$

The augmented autocorrelation matrix $\hat{R}_{yy}^{(\mathbf{n+1})}$ in (25) can be written more explicitly by defining

$$\mathbf{R}_{yy}^{(\mathbf{n})} = E[\mathbf{Y}_{QP}^{(\mathbf{n})} \mathbf{Y}_{QP}^{(\mathbf{n})^T}]$$

$$\hat{\mathbf{R}}_{yy}^{(\mathbf{n})} = \mathbf{U} \otimes \mathbf{R}_{yy}^{(\mathbf{n})} \tag{26a}$$

where $\mathbf{U}$ is a 4×4 matrix with all entries equal to unity and $\otimes$ denotes the Kronecker product [26]. The block toeplitz matrix $\mathbf{R}^{(\mathbf{n})}$ is given by

$$\mathbf{R}_{yy}^{(\mathbf{n})} = \begin{bmatrix} \mathbf{R}_0^{(\mathbf{n})} & \mathbf{R}_1^{(\mathbf{n})} & \cdots & \mathbf{R}_{n_1}^{(\mathbf{n})} \\ \mathbf{R}_{-1}^{(\mathbf{n})} & \mathbf{R}_0^{(\mathbf{n})} & & \\ \vdots & & & \mathbf{R}_1^{(\mathbf{n})} \\ \mathbf{R}_{-n_1}^{(\mathbf{n})} & \cdots & \cdots \mathbf{R}_{-1}^{(\mathbf{n})} & \mathbf{R}_0^{(\mathbf{n})} \end{bmatrix} \tag{26b}$$

with

$$\mathbf{R}_p^{(\mathbf{n})} = \begin{bmatrix} r_{yy}(p,0) & r_{yy}(p,1) & \cdots & r_{yy}(p,n_2) \\ r_{yy}(p,-1) & r_{yy}(p,0) & \cdots & r_{yy}(p,n_2-1) \\ \vdots & & & \vdots \\ & & & r_{yy}(p,1) \\ r_{yy}(p,-n_2) & \cdots & r_{yy}(p,-1) & r_{yy}(p,0) \end{bmatrix} \tag{26c}$$

and

$$\mathbf{R}_{-p}^{(\mathbf{n})} = \mathbf{R}_p^{(\mathbf{n})^T}, \quad p = 0,1,2,\ldots,n_1 \tag{26d}$$

where

$$[r_{yy}(p,q)]_{p,q=-P,-Q}^{P,Q}$$

is the given finite lag autocorrelation matrix.

From Table 1, (25) and (26), one can readily see that the 2-D lattice parameters can be computed from the autocorrelation matrix of the given process and updated coefficients of the forward[2] prediction filter, $\hat{w}_{b_{0,0}}^{(\mathbf{n})}$.

B. Computational Issues

The direct calculation of the error correlation matrix in (25) requires approximately $64n_1^3n_2^3$ computations. However, by considering the symmetry of $\psi_{QP}^{(\mathbf{n})}$ along with block toeplitz property of $\mathbf{R}_{yy}^{(\mathbf{n})}$ and toeplitz form of $\mathbf{R}_p^{(\mathbf{n})}, p = 0,1,\ldots,n_1$, computational complexity can be reduced substantially.

Due to the symmetry in $\psi_{QP}^{(\mathbf{n})}$ only ten prediction error autocorrelation (or crosscorrelation) are needed. For this purpose, define

$$\phi_{e_{i,j}e_{p,q}}^{(\mathbf{n})}(i-p,j-q) = E[e_{i,j}^{(\mathbf{n})}(k_1-i,k_2-j)e_{p,q}^{(\mathbf{n})}(k_1-p,k_2-q)]; (i,j),(p,q) \in D_{QP} \tag{27}$$

[2] In [25], the first prediction error field $e_{0,0}$ is named as forward prediction error field. $e_{1,0}, e_{1,1}$ and $e_{0,1}$ are the backward fields.

From (25) and (26), $\phi^{(\mathbf{n})}_{e_{i,j}e_{p,q}}(i-p,j-q)$ can be rewritten as

$$\phi^{(\mathbf{n})}_{e_{i,j}e_{p,q}}(i-p,j-q) = \hat{\mathbf{W}}^{(\mathbf{n})^T}_{b_{0,0}} \hat{\mathbf{I}}^T_{i,j} \mathbf{R}^{(\mathbf{n+1})}_{yy} \hat{\mathbf{I}}_{p,q} \hat{\mathbf{W}}^{(\mathbf{n})}_{b_{0,0}} \tag{28}$$

from (21a), (28) becomes

$$\phi^{(\mathbf{n})}_{e_{i,j}e_{p,q}}(i-p,j-q) = \hat{\mathbf{W}}^{(\mathbf{n})^T}_{b_{i,j}} \mathbf{R}^{(\mathbf{n+1})}_{yy} \hat{\mathbf{W}}^{(\mathbf{n})}_{p,q} \tag{29}$$

since $\mathbf{R}^{(\mathbf{n+1})}_{yy}$ is block toeplitz and from (26b) $\mathbf{R}^{(\mathbf{n})^T}_{p} = \mathbf{R}^{(\mathbf{n})}_{-p}$, $p = 0, 1, \ldots, n_1$; (29) is written as

$$\begin{aligned}
\phi^{(\mathbf{n})}_{e_{i,j}e_{p,q}}(i-p,j-q) \;=\; & \sum_{l=0}^{n_1+1} \hat{\mathbf{b}}^{(\mathbf{n})^T}_{i,j}(l) \mathbf{R}^{(\mathbf{n+1})}_{0} \hat{\mathbf{b}}^{(\mathbf{n})}_{p,q}(l) \\
& + \sum_{l=0}^{n_1+1} \sum_{k=0}^{n_1+1-k} \Big[\hat{\mathbf{b}}^{(\mathbf{n})^T}_{i,j}(l) \mathbf{R}^{(\mathbf{n+1})}_{l} \hat{\mathbf{b}}^{(\mathbf{n})}_{p,q}(l+k) \\
& + \hat{\mathbf{b}}^{(\mathbf{n})^T}_{i,j}(l+k) \mathbf{R}^{(\mathbf{n+1})}_{-l} \hat{\mathbf{b}}^{(\mathbf{n})}_{p,q}(l) \Big]
\end{aligned} \tag{30}$$

From (26c), each of the internal multiplications can be further simplified by considering the toeplitz property of $\mathbf{R}_p, p = -n_1 - 1, \ldots, n_1 + 1$

$$\begin{aligned}
\hat{\mathbf{b}}^{(\mathbf{n})^T}_{i,j}(m) \mathbf{R}^{(\mathbf{n+1})}_{k} \hat{\mathbf{b}}^{(\mathbf{n})}_{p,q}(n) \;=\; & r_{yy}(k,0) \sum_{t=0}^{n_2+1} \hat{\mathbf{b}}^{(\mathbf{n})}_{i,j}(m,t) \hat{\mathbf{b}}^{(\mathbf{n})}_{p,q}(n,t) \\
& + \sum_{w=0}^{n_2+1} r_{yy}(k,w) \sum_{t=0}^{n_2+1-w} \hat{\mathbf{b}}^{(\mathbf{n})}_{i,j}(m,t) \hat{\mathbf{b}}^{(\mathbf{n})}_{p,q}(n,t+w) \\
& + \sum_{w=0}^{n_2+1} r_{yy}(k,-w) \sum_{t=0}^{n_2+1-w} \hat{\mathbf{b}}^{(\mathbf{n})}_{i,j}(m,t+w) \hat{\mathbf{b}}^{(\mathbf{n})}_{p,q}(n,t)
\end{aligned} \tag{31}$$

Applying the symmetry property of the given autocorrelation; i.e. $r_{yy}(p,q) = r_{yy}(-p,-q)$ and substituting (31) into (30) gives the final equation in (32). For convenience superscript $(\mathbf{n})$ on $b_{i,j}$ and $b_{p,q}$ can be dropped.

$$\begin{aligned}
\phi^{(\mathbf{n})}_{e_{i,j}e_{p,q}}(i-p,j-q) \;=\; & \sum_{m=0}^{n_1+1} \sum_{t=0}^{n_2+1} r_{yy}(0,0) \hat{\mathbf{b}}_{i,j}(m,t) \hat{\mathbf{b}}_{p,q}(m,t) \\
& + \sum_{k=1}^{n_1+1} \sum_{m=0}^{n_1+1-k} \sum_{t=0}^{n_2+1} r_{yy}(k,0) \Big(\hat{\mathbf{b}}_{i,j}(m,t) \hat{\mathbf{b}}_{p,q}(m+k,t) + \hat{\mathbf{b}}_{i,j}(m+k,t) \hat{\mathbf{b}}_{p,q}(m,t) \Big) \\
& + \sum_{m=0}^{n_1+1} \sum_{w=1}^{n_1+1} \sum_{t=0}^{n_2+1-w} r_{yy}(0,w) \Big(\hat{\mathbf{b}}_{i,j}(m,t) \hat{\mathbf{b}}_{p,q}(m,t+w) + \hat{\mathbf{b}}_{i,j}(m,t+w) \hat{\mathbf{b}}_{p,q}(m,t) \Big) \\
& + \sum_{k=1}^{n_1+1} \sum_{m=0}^{n_1+1-k} \sum_{w=1}^{n_2+1} \sum_{t=0}^{n_1+1-w} \Big[r_{yy}(k,w) \Big(\hat{\mathbf{b}}_{i,j}(m,t) \hat{\mathbf{b}}_{p,q}(m+k,t+w) \\
& \hat{\mathbf{b}}_{i,j}(m+k,t+w) \hat{\mathbf{b}}_{p,q}(m,t) \Big) + \\
& r_{yy}(k,-w) \Big(\hat{\mathbf{b}}_{i,j}(m,t+w) \hat{\mathbf{b}}_{p,q}(m+k,t) + \hat{\mathbf{b}}_{i,j}(m+k,t) \hat{\mathbf{b}}_{p,q}(m,t+w) \Big) \Big]
\end{aligned} \tag{32}$$

Now, the computation of $\psi^{(\mathbf{n})}_{QP}$ in (25) with (32) requires approximately $10 n_1^2 n_2^2$ computations.

4. Asymmetric Half-Plane Autoregressive Lattice Modelling

In this section, two asymmetric half-plane autoregressive models are proposed for modelling of a random field from its given autocorrelation matrix. The first model is recursive row by row and reported earlier [27]. The

second model is given in this paper and recursive column by column. It will be shown by numerical examples that these AR lattice models may lead to different results because of geometry of their error prediction mask.

A. Model 1

The prediction error fields are defined by the following equation [27]:

$$\mathbf{e}_{HP_1}^{(\mathbf{n+1})}(k_1,k_2) = \mathbf{K}_{HP_1}^{(\mathbf{n+1})}\mathbf{e}_{HP_1}^{(\mathbf{n})}(k_1,k_2)^* \tag{33a}$$

with the following initial conditions;

$$e_{i,j}^{(0,0)}(k_1,k_2) = y(k_1,k_2), \quad (i,j) \in D_{HP_1} \tag{33b}$$

where

$$D_{HP_1} = \{(0,0),(1,0),(1,1),(0,1),(1,-1)\} \tag{33c}$$

$$\mathbf{e}_{HP_1}^{(\mathbf{n})}(k_1,k_2) = \left[\mathbf{e}_{QP}^{(\mathbf{n})^T}(k_1,k_2) \vdots e_{HP_1}^{(\mathbf{n})}(k_1,k_2)\right]^T \tag{33d}$$

$$\mathbf{e}_{HP_1}^{(\mathbf{n})}(k_1,k_2)^* = \left[\mathbf{e}_{QP}^{(\mathbf{n})^T}(k_1,k_2) \vdots e_{HP_1}^{(\mathbf{n})}(k_1-1,k_2+1)\right]^T \tag{33e}$$

and

$$\mathbf{K}_{HP_1}^{(\mathbf{n})} = \mathbf{I} - k_{1,0}^{(\mathbf{n})}\mathbf{P}_{1,0} - k_{1,1}^{(\mathbf{n})}\mathbf{P}_{1,1} - k_{0,1}^{(\mathbf{n})}\mathbf{P}_{0,1} - k_{1,-1}^{(\mathbf{n})}\mathbf{P}_{1,-1} \tag{33f}$$

with

$$\mathbf{P}_{1,0} = \left[\begin{array}{cccc|c} & \mathbf{P} & & & \mathbf{O} \\ \cdots & \cdots & \cdots & \cdots & \cdots \\ 0 & 1 & 0 & 0 & 0 \end{array}\right]; \mathbf{P}_{1,1} = \left[\begin{array}{cccc|c} & \tilde{\mathbf{P}} & & & \mathbf{O} \\ \cdots & \cdots & \cdots & \cdots & \cdots \\ 0 & 0 & 1 & 0 & 0 \end{array}\right]; \tag{33g}$$

$$\mathbf{P}_{0,1} = \left[\begin{array}{cccc|c} & \tilde{\mathbf{I}} & & & \mathbf{O} \\ \cdots & \cdots & \cdots & \cdots & \cdots \\ 0 & 0 & 0 & 1 & 0 \end{array}\right]; \mathbf{P}_{1,-1} = \left[\begin{array}{cccc|c} & & & & 1 \\ & & & & 1 \\ & \mathbf{O} & & & 1 \\ & & & & 1 \\ \cdots & \cdots & \cdots & \cdots & \cdots \\ 1 & 0 & 0 & 0 & 0 \end{array}\right]; \tag{33h}$$

The prediction error vector $\mathbf{e}_{QP}^{(\mathbf{n})}(k_1,k_2)$ and permutation matrices $\mathbf{P}, \tilde{\mathbf{I}}$, and $\tilde{\mathbf{P}}$ are defined in (13) for the quarter-plane case. It is interesting to note that if the lattice parameter value $k_{1,-1} = 0$ then (33a)-(33g) reduce to the quarter-plane model in (13). This property indicates that asymmetric half-plane model contains quarter-plane model.

Starting with the given initial random field, $e_{i,j}^{(\mathbf{0})} = y(k_1,k_2)$, $(i,j) \in D_{HP_1}$, the data of these five fields are then combined linearly to calculate the prediction error fields of successively higher order lattice stages. The generation of prediction error fields is shown in Fig. 4. Starting with five data points in the upper left hand corner of each of the five fields; $e_{i,j}^{(\mathbf{n-1})}(k_1,k_2), (i,j) \in D_{HP_1}$; the data is processed as indicated in Fig. 5 to calculate the five prediction error fields of the next higher $(\mathbf{n})$-th order lattice model.

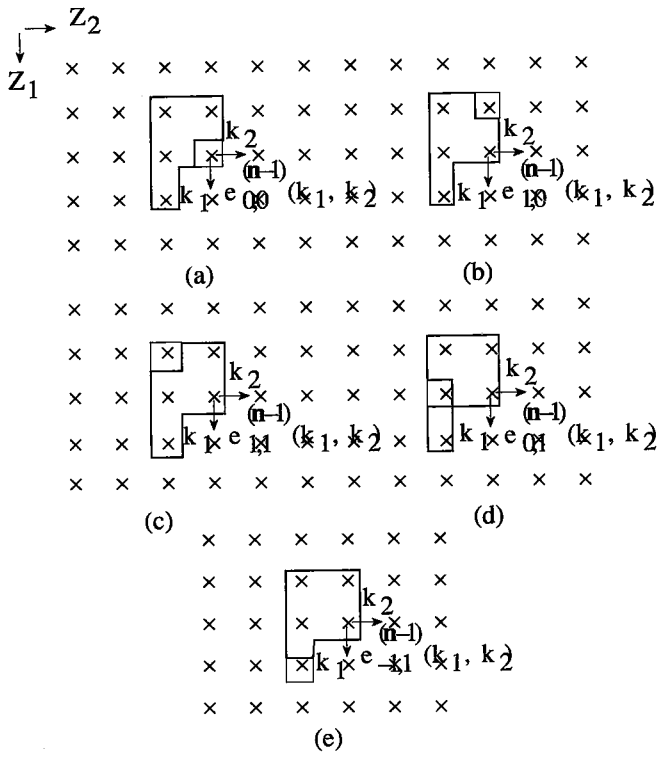

Figure 4. The asymmetric half-plane (Model 1) error fields of order $(\mathbf{n}-\mathbf{1})$ used to generate prediction error fields of order $(\mathbf{n})$.

The calculation of the four lattice parameter reflection factors at each stage is similar to the quarter-plane model in Section 3. The following mean-squared error is defined by $(\mathbf{n}+1)$-th order lattice model

$$Q_{HP}^{(\mathbf{n+1})} = \text{trace}\left[\mathbf{e}_{HP_1}^{(\mathbf{n+1})}(k_1,k_2)\mathbf{\Lambda}_{DH}\mathbf{e}_{HP_1}^{(\mathbf{n+1})^T}(k_1,k_2)\right] \tag{34}$$

where

$$\mathbf{\Lambda}_{DH} = \text{diag.matrix}\left[\lambda_1\ \lambda_2\ \lambda_3\ \lambda_4\ \lambda_5\right].$$

The λ_i, $i = 1,2,\ldots,5$, are arbitrary weights taken to be either 0 or 1, to be associated with the expected values of the five prediction error fields in (33a). Similar to (15a), the results of this minimization are summarized in the following equation

$$\mathbf{R}_{HP_1}^{(\mathbf{n})}\mathbf{k}_{HP_1}^{(\mathbf{n+1})} = \mathbf{r}_{HP_1}^{(\mathbf{n})} \tag{35}$$

where $\mathbf{R}_{HP_1}^{(\mathbf{n})}$ and $\mathbf{r}_{HP_1}^{(\mathbf{n})}$ are the symmetric correlation matrix and vector with an order of 4×4 and 4×1 respectively. $\mathbf{k}_{HP_1}^{(\mathbf{n})}$ is defined as

$$\mathbf{k}_{HP_1}^{(\mathbf{n})} = \left[\mathbf{k}_{QP}^{(\mathbf{n})^T} : k_{1,-1}^{(\mathbf{n})}\right]^T \tag{36}$$

Substituting (33a) into (34) and simplifying the result yields

$$\mathbf{Q}_{HP_1}^{(\mathbf{n+1})} = \mathbf{Q}_{HP_1}^{(\mathbf{n})} - \frac{1}{2}\mathbf{k}_{HP_1}^{(\mathbf{n+1})^T}\mathbf{R}_{HP_1}^{(\mathbf{n})}\mathbf{k}_{HP_1}^{(\mathbf{n+1})} \tag{37}$$

as in the quarter-plane model, if the correlation matrix $\mathbf{R}_{HP_1}^{(\mathbf{n})}$ is positive definite, the minimum mean square prediction error will decrease with successive stages.

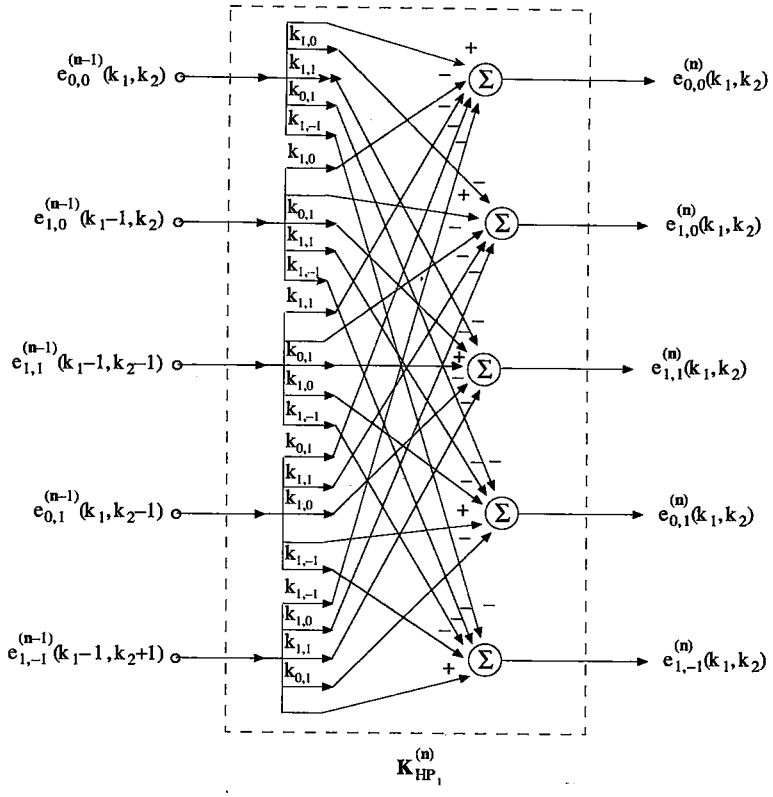

Figure 5. The analysis model for the asymmetric half-plane (Model 1).

The components of $\mathbf{R}^{(\mathbf{n})}_{HP_1}$ and $\mathbf{r}^{(\mathbf{n})}_{HP_1}$ are given in Table 2. In the following section, it will be shown that it is also possible to express the error correlation matrix $\psi^{(\mathbf{n})}_{HP_1}$ in terms of the sums of the weighted present and past values of the data field in (17).

From (33), the prediction error fields can be written as

$$e^{(\mathbf{n})}_{i,j}(k_1,k_2) = \mathbf{Y}^{(\mathbf{n})^T}_{HP_1}\mathbf{W}^{(\mathbf{n})}_{b_{i,j}}, \quad (i,j) \in D_{HP_1} \tag{38a}$$

where

$$\mathbf{Y}^{(\mathbf{n})}_{HP_1} = \left[y^{(\mathbf{n})^T}_{HP_1}(O)\vdots\cdots\vdots y^{(\mathbf{n})^T}_{HP_1}(n_1)\right]^T \tag{38b}$$

$$\mathbf{W}^{(\mathbf{n})}_{b_{i,j}} = \left[\mathbf{b}^{(\mathbf{n})^T}_{i,j}(O)\vdots\cdots\vdots\mathbf{b}^{(\mathbf{n})^T}_{i,j}(n_1)\right]^T \tag{38c}$$

with

$$\mathbf{Y}^{(\mathbf{n})}_{HP_1}(l) = [y(k_1-l,k_2+n_2)\cdots y(k_1-l,k_2)\cdots y(k_1-l,k_2-n_2)]^T \tag{38d}$$

$$b^{(\mathbf{n})}_{i,j}(l) = \left[b^{(\mathbf{n})}_{i,j}(l,-n_2)\cdots b^{(\mathbf{n})}_{i,j}(l,0)\cdots b^{(\mathbf{n})}_{i,j}(l,n_2)\right]^T \tag{38e}$$

$$l = 0,1,\ldots,n_1$$

where

$$\left[b^{(\mathbf{n})}_{i,j}(p,q)\right]^{n_1,n_2}_{p=q,q=n_2}; \quad (i,j) \in D_{HP_1}$$

is the coefficient matrix of the prediction error transfer function $B^{(\mathbf{n})}_{i,j}(z_1,z_2)$ defined in (19a).

Table 2. Prediction Error Covariances for the Half-Plane Model

$R_{11}^{(\mathbf{n})}$	$\psi_{HP}^{(\mathbf{n})} o[2\mathbf{P}_{1,0}^T \mathbf{\Lambda}_{DH} \mathbf{P}_{1,0}]$
$R_{12}^{(\mathbf{n})}$	$\psi_{HP}^{(\mathbf{n})} o[\mathbf{P}_{1,0}^T \mathbf{\Lambda}_{DH} \mathbf{P}_{1,1} + \mathbf{P}_{1,1}^T \mathbf{\Lambda}_{DH} \mathbf{P}_{1,0}]$
$R_{13}^{(\mathbf{n})}$	$\psi_{HP}^{(\mathbf{n})} o[\mathbf{P}_{1,0}^T \mathbf{\Lambda}_{DH} \mathbf{P}_{0,1} + \mathbf{P}_{0,1}^T \mathbf{\Lambda}_{DH} \mathbf{P}_{1,0}]$
$R_{14}^{(\mathbf{n})}$	$\psi_{HP}^{(\mathbf{n})} o[\mathbf{P}_{1,0}^T \mathbf{\Lambda}_{DH} \mathbf{P}_{1,-1} + \mathbf{P}_{1,-1}^T \mathbf{\Lambda}_{DH} \mathbf{P}_{1,0}]$
$R_{14}^{(\mathbf{n})}$	$\psi_{HP}^{(\mathbf{n})} o[\mathbf{P}_{1,0}^T \mathbf{\Lambda}_{DH} \mathbf{P}_{1,-1} + \mathbf{P}_{1,-1}^T \mathbf{\Lambda}_{DH} \mathbf{P}_{1,0}]$
$R_{22}^{(\mathbf{n})}$	$\psi_{HP}^{(\mathbf{n})} o[2\mathbf{P}_{1,1}^T \mathbf{\Lambda}_{DH} \mathbf{P}_{1,1}]$
$R_{23}^{(\mathbf{n})}$	$\psi_{HP}^{(\mathbf{n})} o[\mathbf{P}_{1,1}^T \mathbf{\Lambda}_{DH} \mathbf{P}_{0,1} + \mathbf{P}_{0,1}^T \mathbf{\Lambda}_{DH} \mathbf{P}_{1,1}]$
$R_{33}^{(\mathbf{n})}$	$\psi_{HP}^{(\mathbf{n})} o[2\mathbf{P}_{0,1}^T \mathbf{\Lambda}_{D} H \mathbf{P}_{0,1}]$
$R_{34}^{(\mathbf{n})}$	$\psi_{HP}^{(\mathbf{n})} o[\mathbf{P}_{0,1}^T \mathbf{\Lambda}_{DH} \mathbf{P}_{1,-1} + \mathbf{P}_{1,-1}^T \mathbf{\Lambda}_{DH} \mathbf{P}_{0,1}]$
$R_{44}^{(\mathbf{n})}$	$\psi_{HP}^{(\mathbf{n})} o[2\mathbf{P}_{1,-1}^T \mathbf{\Lambda}_{DH} \mathbf{P}_{1,-1}]$
$R_{11}^{(\mathbf{n})}$	$\psi_{HP}^{(\mathbf{n})} o[\mathbf{P}_{1,0}^T \mathbf{\Lambda}_{DH} + \mathbf{\Lambda}_{DH} \mathbf{P}_{1,0}]$
$R_{21}^{(\mathbf{n})}$	$\psi_{HP}^{(\mathbf{n})} o[\mathbf{P}_{1,1}^T \mathbf{\Lambda}_{DH} + \mathbf{\Lambda}_{DH} \mathbf{P}_{1,1}]$
$R_{31}^{(\mathbf{n})}$	$\psi_{HP}^{(\mathbf{n})} o[\mathbf{P}_{0,1}^T \mathbf{\Lambda}_{DH} + \mathbf{\Lambda}_{DH} \mathbf{P}_{0,1}]$
$R_{41}^{(\mathbf{n})}$	$\psi_{HP}^{(\mathbf{n})} o[\mathbf{P}_{1,-1}^T \mathbf{\Lambda}_{DH} + \mathbf{\Lambda}_{DH} \mathbf{P}_{1,-1}]$

Then, the shifted prediction error vector, $\mathbf{e}_{HP_1}^{(\mathbf{n})}(k_1, k_2)^*$ in (33e) can be written as

$$e_{i,j}^{(\mathbf{n})}(k_1 - i, k_2 - j) = \mathbf{Y}_{HP_1}^{(\mathbf{n}+\mathbf{1})^T} \hat{\mathbf{W}}_{b_{i,j}}^{(\mathbf{n})} \quad (i,j) \in D_{HP_1} \tag{39}$$

where

$$\hat{\mathbf{W}}_{b_{0,0}}^{(\mathbf{n})} = \left[\mathbf{O}^T \vdots \hat{\mathbf{b}}_{0,0}^{(\mathbf{n})^T}(O) \vdots \cdots \vdots \hat{\mathbf{b}}_{0,0}^{(\mathbf{n})^T}(n_1)\right] \tag{40a}$$

$$\hat{\mathbf{W}}_{b_{1,0}}^{(\mathbf{n})} = \left[\hat{\mathbf{b}}_{1,0}^{(\mathbf{n})^T}(O) \vdots \cdots \vdots \hat{\mathbf{b}}_{1,0}^{(\mathbf{n})^T}(n_1) \vdots \mathbf{O}^T\right] \tag{40b}$$

$$\hat{\mathbf{W}}_{b_{1,1}}^{(\mathbf{n})} = \left[\hat{\mathbf{b}}_{1,1}^{(\mathbf{n})^T}(O) \vdots \cdots \vdots \hat{\mathbf{b}}_{1,1}^{(\mathbf{n})^T}(n_1) \vdots \mathbf{O}^T\right] \tag{40c}$$

$$\hat{\mathbf{W}}_{b_{0,1}}^{(\mathbf{n})} = \left[\mathbf{O}^T \vdots \hat{\mathbf{b}}_{0,1}^{(\mathbf{n})^T}(O) \vdots \cdots \vdots \hat{\mathbf{b}}_{0,1}^{(\mathbf{n})^T}(n_1)\right] \tag{40d}$$

$$\hat{\mathbf{W}}_{b_{1,-1}}^{(\mathbf{n})} = \left[\mathbf{O}^T \vdots \hat{\mathbf{b}}_{1,-1}^{(\mathbf{n})^T}(O) \vdots \cdots \vdots \hat{\mathbf{b}}_{1,-1}^{(\mathbf{n})^T}(n_1)\right] \tag{40e}$$

with

$$\hat{\mathbf{b}}_{0,0}^{(\mathbf{n})}(l) = \left[O \vdots \mathbf{b}_{0,0}^{(\mathbf{n})^T}(l) \vdots O\right]^T \tag{41a}$$

$$\hat{\mathbf{b}}_{1,0}^{(\mathbf{n})}(l) = \left[O \vdots \mathbf{b}_{1,0}^{(\mathbf{n})^T}(l) \vdots O\right]^T \tag{41b}$$

$$\hat{\mathbf{b}}_{1,1}^{(\mathbf{n})}(l) = \left[O \vdots O \vdots \mathbf{b}_{1,1}^{(\mathbf{n})^T}(l)\right] \tag{41c}$$

$$\hat{\mathbf{b}}_{0,1}^{(\mathbf{n})}(l) = \left[O \vdots O \vdots \mathbf{b}_{0,1}^{(\mathbf{n})^T}(l)\right] \tag{41d}$$

$$\hat{\mathbf{b}}_{1,-1}^{(\mathbf{n})}(l) = \left[\mathbf{b}_{1,-1}^{(\mathbf{n})^T}(l) \vdots O \vdots O\right] \tag{41e}$$

$$l = 0, 1, 2, \ldots, n_1$$

Then, $\psi_{HP_1}^{(\mathbf{n})}$ matrix in Table 2, can be written by using (39) as

$$\begin{aligned} \psi_{HP_1}^{(\mathbf{n})} &= \left[\mathbf{e}_{HP_1}^{(\mathbf{n})}(k_1,k_2)^* \mathbf{e}_{HP_1}^{(\mathbf{n})^T}(k_1,k_2)^*\right] \\ &= \widehat{\widehat{\mathbf{W}}}^{\mathbf{n}^T} \hat{\hat{\mathbf{R}}}^{(\mathbf{n+1})} \widehat{\widehat{\mathbf{W}}}^{\mathbf{n}} \end{aligned} \tag{42}$$

with

$$\widehat{\widehat{\mathbf{W}}} = \left[\mathbf{W}_{b_{0,0}}^{(\mathbf{n})} \vdots \mathbf{W}_{b_{1,0}}^{(\mathbf{n})} \vdots \mathbf{W}_{b_{1,1}}^{(\mathbf{n})} \vdots \mathbf{W}_{b_{0,1}}^{(\mathbf{n})} \vdots \mathbf{W}_{b_{1,-1}}^{(\mathbf{n})}\right]^T$$

where $\hat{\hat{\mathbf{R}}}_{yy}^{(\mathbf{n})}$ is a block matrix as in (26a) with an order of $5(n_1+1)(2n_2+1) \times 5(n_1+1)(2n_2+1)$. Each block matrix is denoted as $\tilde{\mathbf{R}}_{yy}^{(\mathbf{n})}$ where

$$\tilde{\mathbf{R}}_{yy}^{(\mathbf{n})} = \begin{bmatrix} \tilde{\mathbf{R}}_0^{(\mathbf{n})} & \tilde{\mathbf{R}}_1^{(\mathbf{n})} & \cdots & \tilde{\mathbf{R}}_{n_1}^{(\mathbf{n})} \\ \tilde{\mathbf{R}}_{-1}^{(\mathbf{n})} & \tilde{\mathbf{R}}_0^{(\mathbf{n})} & & \vdots \\ \vdots & & & \tilde{\mathbf{R}}_1^{(\mathbf{n})} \\ \tilde{\mathbf{R}}_{-n_1}^{(\mathbf{n})} & \cdots & \tilde{\mathbf{R}}_{-1}^{(\mathbf{n})} & \tilde{\mathbf{R}}_0^{(\mathbf{n})} \end{bmatrix} \tag{43a}$$

with

$$\mathbf{R}_i^{(\mathbf{n})} = \begin{bmatrix} r_{yy}(i,0) & r_{yy}(i,1) & \cdots & r_{yy}(i,2n_2-1) & r_{yy}(i,2n_2) \\ r_{yy}(i,-1) & r_{yy}(i,0) & & & r_{yy}(i,2n_2-1) \\ \vdots & & & & \vdots \\ r_{yy}(i,-2n_2+1) & & & & r_{yy}(i,1) \\ r_{yy}(i,-2n_2) & \cdots & & r_{yy}(i,-1) & r_{yy}(i,0) \end{bmatrix} \tag{43b}$$

and

$$\tilde{\mathbf{R}}_{-i}^{(\mathbf{n})} = \tilde{\mathbf{R}}_i^{(\mathbf{n})^T} \tag{43c}$$

The direct calculation of the $\psi_{HP_1}^{(\mathbf{n})}$ in (42) requires approximately $5^3 n_1^3 (2n_2)^3$ computations. As in the quarter-plane case discussed in Section 3-B, symmetry and block toeplitz properties reduce the number of computations to approximately $15 n_1^2 (2n_2)^2$. The final equation to calculate is the same as in (32). (n_2+1) term in the upper bounds of the summations will be doubled; i.e., $2(n_2+1)$. However, a different updating procedure is necessary to update the coefficients at each stage.

From (42) and Table 2, it is clear that it is possible to calculate lattice parameter factors from the given autocorrelation matrix and the updated weighting sequences.

B. Model 2

The first four prediction error fields of this model are the same as in Model 1 given in previous section. The prediction error fields are defined by the following equation

$$\mathbf{e}_{HP_2}^{(\mathbf{n+1})}(k_1,k_2) = \mathbf{K}_{HP_2}^{(\mathbf{n+1})}\mathbf{e}_{HP_2}^{(\mathbf{n})}(k_1,k_2)^* \tag{44a}$$

with

$$e_{i,j}^{(\mathbf{O})}(k_1,k_2) = y(k_1,k_2); \quad (i,j) \in D_{HP_2} \tag{44b}$$

where

$$D_{HP_2} = \{(0,0),(1,0),(1,1),(0,1),(-1,1)\} \tag{44c}$$

$$e_{HP_2}^{(\mathbf{n})}(k_1,k_2) = \left[\mathbf{e}_{QP}^{(\mathbf{n})^T}(k_1,k_2) \vdots e_{-1,1}^{(\mathbf{n})}(k_1,k_2)\right]^T \tag{44d}$$

$$e_{HP_2}^{(\mathbf{n})}(k_1,k_2) = \left[\mathbf{e}_{QP}^{(\mathbf{n})^T}(k_1,k_2) \vdots e_{-1,1}^{(\mathbf{n})}(k_1+1,k_2-1)\right]^T \tag{44e}$$

and

$$\mathbf{K}_{HP_2}^{(\mathbf{n})} = \mathbf{I} - k_{1,0}^{(\mathbf{n})}\mathbf{P}_{1,0} - k_{1,1}^{(\mathbf{n})}\mathbf{P}_{1,1} - k_{0,1}^{(\mathbf{n})}\mathbf{P}_{0,1} - k_{1,1}^{(\mathbf{n})}\mathbf{P}_{-1,1} \tag{44f}$$

with

$$\mathbf{P}_{-1,1} = \mathbf{P}_{1,-1}$$

given in (33g).

The generation of prediction error fields is shown in Fig. 6. The forward prediction error, $e_{0,0}(k_1,k_2)$ is generated autoregressively using all data on columns to the left of the point being estimated and data at the top of the point on the same line. This corresponds to normal raster scanning of an image starting at the upper left hand corner proceeding top to bottom, left to right.

Since all other aspects of Model 1 and Model 2, are identical repetition will be avoided. The only difference comes from the support of the coefficients of the prediction error fields which is given in Fig. 7. The equation in (32) can be used to compute the prediction error correlations by changing (n_1+1) in the upper bounds to $(2n_1+1)$.

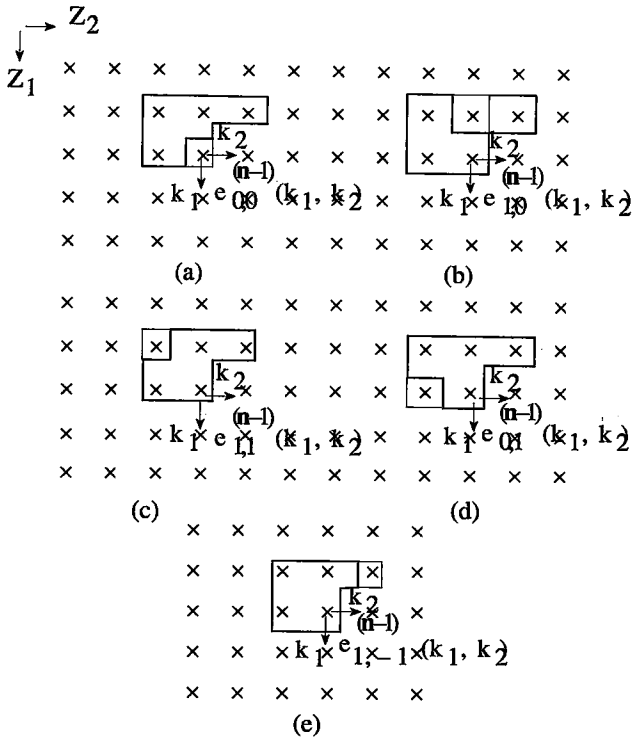

Figure 6. The asymmetric half-plane (Model 2) error fields of order $(\mathbf{n}-\mathbf{1})$ used to generate prediction error fields of order $(\mathbf{n})$.

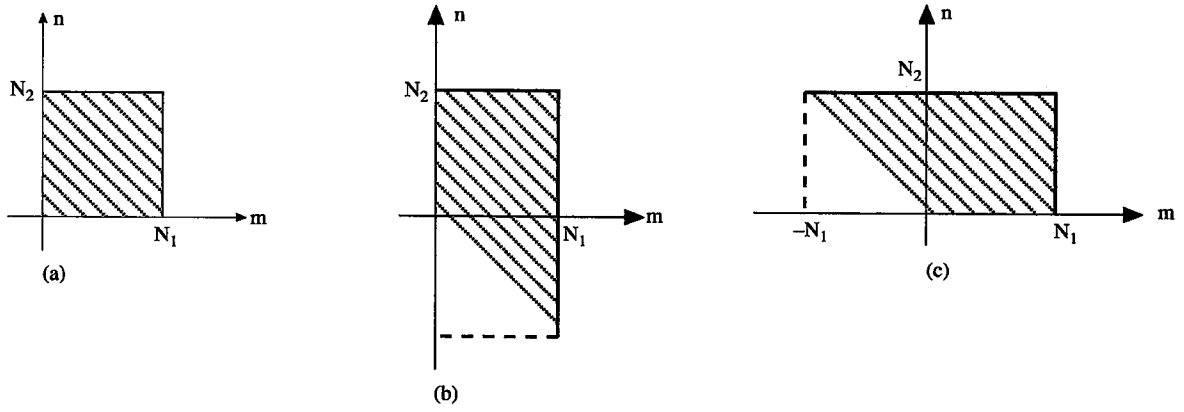

Figure 7. Support domain for the coefficients of the transfer function; (a) quarter-plane, (b) Model 1, (c) Model 2.

5. The Synthesis Model Conditions for Lattice Model Stability

For both quarter-plane and asymmetric half-plane model, it was shown [25], [27] that it is possible to invert the lattice structure into a synthesis model which is capable of generating the original field $y(k_1,k_2) = e_{i,j}^{(\mathbf{O})}(k_1,k_2)$, from an input field,

$$u(k_1,k_2) = e_{0,0}^{(\mathbf{N})}(k_1,k_2).$$

If the lattice parameters have to be calculated using sufficient stages so that the prediction error fields in the last $(\mathbf{N})$-th stage are white noise, then $u(k_1,k_2)$ is a white noise field. The synthesis algorithms can be obtained by partitioning equations (13a), (33a), and (44a) for all three models [25], [27].

Fig. 8 illustrates a succession of cascaded synthesis model stages for the quarter-plane case. Starting with

$$u(k_1,k_2) = e_{0,0}^{(\mathbf{N})}(k_1,k_2)$$

as a random 2-D white noise field, assuming zero initial conditions for all of the backward prediction error fields, it is possible to process the 2-D data along rows (or columns) to produce the original field $\mathbf{Y}(k_1,k_2)$.

The synthesis model algorithm structure (synthesis model) can be obtained by rearranging the first equation of (13a).

$$\begin{bmatrix} e_{0,0}^{(\mathbf{N-1})}(k_1,k_2) \\ e_{1,0}^{(\mathbf{N})}(k_1,k_2) \\ e_{1,1}^{(\mathbf{N})}(k_1,k_2) \\ e_{0,1}^{(\mathbf{N})}(k_1,k_2) \end{bmatrix} = \tilde{\mathbf{K}}_{QP}^{(\mathbf{N})} \begin{bmatrix} e_{0,0}^{(\mathbf{N})}(k_1,k_2) \\ e_{1,0}^{(\mathbf{N-1})}(k_1-1,k_2) \\ e_{1,1}^{(\mathbf{N-1})}(k_1-1,k_2-1) \\ e_{0,1}^{(\mathbf{N-1})}(k_1,k_2-1) \end{bmatrix} \tag{45a}$$

where

$$\tilde{\mathbf{K}}_{QP}^{(\mathbf{n})} = \begin{bmatrix} 1 & +k_{1,0}^{(\mathbf{n})} & +k_{1,1}^{(\mathbf{n})} & +k_{0,1}^{(\mathbf{n})} \\ -k_{1,0}^{(\mathbf{n})} & 1 & -k_{0,1}^{(\mathbf{n})} & -k_{1,1}^{(\mathbf{n})} \\ -k_{1,1}^{(\mathbf{n})} & -k_{0,1}^{(\mathbf{n})} & 1 & -k_{1,0}^{(\mathbf{n})} \\ -k_{0,1}^{(\mathbf{n})} & -k_{1,1}^{(\mathbf{n})} & -k_{1,0}^{(\mathbf{n})} & 1 \end{bmatrix} \tag{45b}$$

$\tilde{\mathbf{K}}_{QP}^{(\mathbf{n})}$ is obtained by changing the signs of lattice parameters of the first row of the analysis model gain matrix $\mathbf{K}_{QP}^{(\mathbf{n})}$.

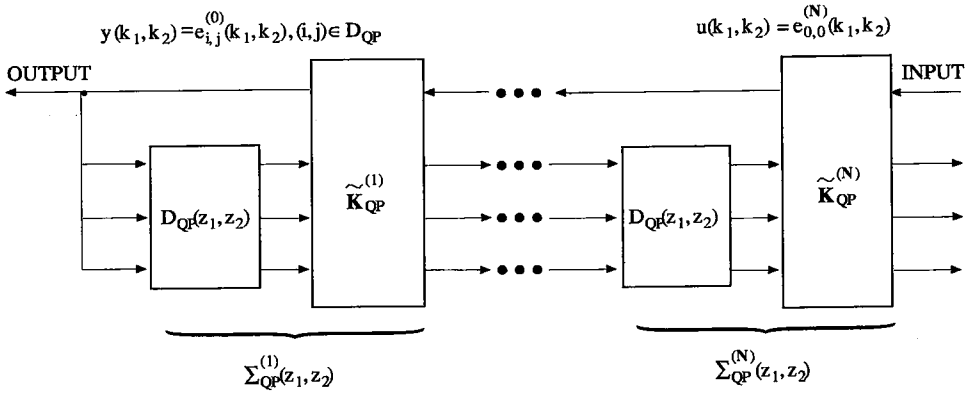

Figure 8. The synthesis model for the quarter-plane case. Its block interconnection is the same as in Fig. 2(b).

The synthesis model for the asymmetric half-plane model (model 1) is given in Fig. 9. The synthesis model equations can be obtained similar to the quarter-plane case. The transfer function of the single stage lattice model is given as

$$\Sigma_{HP_1}^{(\mathbf{n})}(z_1,z_2) = \tilde{\mathbf{K}}_{HP_1}^{(\mathbf{n})} \begin{bmatrix} 1 & \mathbf{O}^T \\ \mathbf{O} & D_{HP_1}(z_1,z_2) \end{bmatrix} \tag{46a}$$

where

$$D_{HP_1}(z_1,z_2) = \text{diag.matrix}\left[z_1^{-1} \;\; (z_1^{-1}z_1^{-1}) \;\; z_1^{-1}(z_1^{-1}z_2)\right] \tag{46b}$$

$\tilde{\mathbf{K}}_{HP_1}^{(\mathbf{n})}$ is the synthesis model gain matrix. It is obtained by changing the signs of lattice parameters of the first row of the analysis model gain matrix $\mathbf{K}_{HP_1}^{(\mathbf{n})}$ in (33f). In this model, it is only possible to process the

data along the columns (row by row recursion). However, the second model in Section 4-B requires column by column recursion [27].

Since the lattice parameter stages are in tandem in the synthesis model a sufficient condition for overall stability of the synthesis model is that each stage be stable. The following stability conditions are obtained for the quarter-plane and the asymmetric half-plane models:

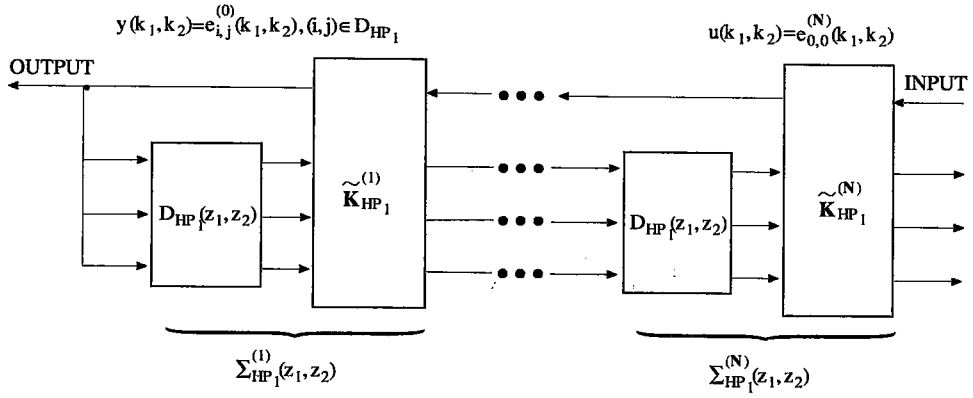

Figure 9. The synthesis model for the asymmetric half-plane (Model 1). Its block interconnection is the same as in Figure 5.

The Necessary and Sufficient Conditions for the Quarter-Plane Model [25]:

$$\text{i)} \quad \left|k_{1,0}^{(\mathbf{n})}\right| < 1 \tag{47a}$$

$$\text{ii)} \quad \left|\frac{k_{1,1}^{(\mathbf{n})} + k_{0,1}^{(\mathbf{n})}}{1 - k_{1,0}^{(\mathbf{n})}}\right| < 1 \tag{47b}$$

$$\text{iii)} \quad \left|\frac{k_{1,1}^{(\mathbf{n})} - k_{0,1}^{(\mathbf{n})}}{1 + k_{1,0}^{(\mathbf{n})}}\right| < \frac{1}{N} \tag{47c}$$

with

$$N = \max[N(w_1, w_2)]$$

where

$$N(w_1, w_2) = \left|\frac{B_{0,0}^{(\mathbf{n})}(z_1, z_2^{-1})}{B_{0,0}^{(\mathbf{n})}(z_1, z_2)}\right|_{|z_1|=|z_2|=1}$$

The Necessary and Sufficient Conditions for the Asymmetric Half-Plane Models:
Model 1 [27]

$$\text{i)} \quad \left|k_{0,1}^{(\mathbf{n})}\right| < 1 \tag{48a}$$

$$\text{ii)} \quad \left|\frac{k_{1,0}^{(\mathbf{n})} + k_{1,1}^{(\mathbf{n})} + k_{1,-1}^{(\mathbf{n})}}{1 - k_{0,1}^{(\mathbf{n})}\, M_{0,1}}\right| < \frac{1}{M_{HP_1}} \tag{48b}$$

with

$$M_{HP_1} = \max[M_{1,0}, M_{1,1}, M_{1,-1}]$$

where

$$M_{i,j} = \max \left| \frac{B_{i,j}(z_1,1)}{B_{0,0}(z_1,1)} \right|_{|z_1|=1} ; (i,j) \in D_{HP_1}$$

$$\text{iii)} \quad \left|k_{1,0}^{(\mathbf{n})}\right| + \left|k_{1,1}^{(\mathbf{n})}\right| + \left|k_{0,1}^{(\mathbf{n})}\right| + \left|k_{1,-1}^{(\mathbf{n})}\right| < \frac{1}{N_{HP_1}} \tag{48c}$$

with

$$N_{HP_1} = \max[N_{1,0}, N_{1,1}, N_{0,1}, N_{1,-1}]$$

where

$$N_{i,j} = \max \left| \frac{B_{i,j}^{(\mathbf{n})}(z_1,z_2)}{B_{0,0}^{(\mathbf{n})}(z_1,z_2)} \right|_{|z_1|=|z_2|=1} ; (i,j) \in D_{HP_1}$$

Model 2:

$$\text{i)} \quad \left|k_{1,0}^{(\mathbf{n})}\right| < 1 \tag{49a}$$

$$\text{ii)} \left| \frac{k_{0,1}^{(\mathbf{n})} + k_{1,1}^{(\mathbf{n})} + k_{-1,1}^{(\mathbf{n})}}{1 - k_{1,0}^{(\mathbf{n})} M_{1,0}} \right| < \frac{1}{M_{HP_2}} \tag{49b}$$

with

$$M_{HP_2} = \max[M_{0,1}, M_{1,1}, M_{-1,1}]$$

where

$$M_{i,j} = \max \left| \frac{B_{i,j}(1,z_2)}{B_{0,0}(1,z_2)} \right|_{|z_2|=1} ; (i,j) \in D_{HP_2}$$

$$\text{iii)} \quad \left|k_{1,0}^{(\mathbf{n})}\right| + \left|k_{1,1}^{(\mathbf{n})}\right| + \left|k_{0,1}^{(\mathbf{n})}\right| + \left|k_{-1,1}^{(\mathbf{n})}\right| < \frac{1}{N_{HP_2}} \tag{49c}$$

with

$$N_{HP_2} = \max[N_{1,0}, N_{1,1}, N_{0,1}, N_{-1,1}]$$

6. Structurally Stable Quarter-Plane Lattice Models

Recent investigations [28] showed that the synthesis filter is stable for every choice of parameters that satisfy the constraint of orthogonality. This is based on a fundamental connection between structural stability and the notions of passivity and losslessness [29]. The constraint for structural stability is given as follows

$$\Sigma^{(\mathbf{n})}(z_1,z_2)\Sigma^{(\mathbf{n})^*}(z_1,z_2) = \mathbf{I}$$

for

$$|z_1| = |z_2| = 1$$

where $\Sigma^{(\mathbf{n})}(z_1,z_2)$ is the scattering matrix describing the n-th section. The asterisk (*) denotes Hermitian transpose (complex conjugate for scalars).

For the quarter-plane lattice model as shown in Fig. 8, the scattering matrix is

$$\Sigma_{QP}^{(\mathbf{n})}(z_1, z_2) = \tilde{\mathbf{K}}_{QP}^{(\mathbf{n})} \begin{bmatrix} 1 & \mathbf{O}^T \\ \mathbf{O} & D_{QP}(z_1, z_2) \end{bmatrix} \tag{50a}$$

where

$$D_{QP}(z_1, z_2) = \text{diag.matrix}\left[z_1^{-1} \;\; (z_1^{-1} z_2^{-1}) \;\; z_2^{-1}\right] \tag{50b}$$

Consequently, the orthogonality requirement of structural stability in (50) is equivalent to

$$\tilde{\mathbf{K}}_{QP}^{(\mathbf{n})} \tilde{\mathbf{K}}_{QP}^{(\mathbf{n})^*} = \mathbf{I} \tag{51}$$

Unfortunately, the 2-D lattice filter presented in Section 3 does not satisfy the constraint in (51). Therefore, it does not have lossless sections, so its structural stability cannot be guaranteed.

To meet the orthogonality requirement we introduce following gain matrices for 2-D quarter-plane lattice filters [31].

$$\tilde{\mathbf{K}}_{QP_1}^{(\mathbf{n})} = \frac{1}{k^{(\mathbf{n})}} \begin{bmatrix} 1 & k_{1,0}^{(\mathbf{n})} & k_{1,1}^{(\mathbf{n})} & k_{0,1}^{(\mathbf{n})} \\ -k_{1,0}^{(\mathbf{n})} & 1 & -k_{0,1}^{(\mathbf{n})} & k_{1,1}^{(\mathbf{n})} \\ k_{1,1}^{(\mathbf{n})} & -k_{0,1}^{(\mathbf{n})} & -1 & k_{1,0}^{(\mathbf{n})} \\ k_{0,1}^{(\mathbf{n})} & k_{1,1}^{(\mathbf{n})} & -k_{1,0}^{(\mathbf{n})} & -1 \end{bmatrix} \tag{52a}$$

$$\tilde{\mathbf{K}}_{QP_2}^{(\mathbf{n})} = \frac{1}{k^{(\mathbf{n})}} \begin{bmatrix} 1 & -k_{1,0}^{(\mathbf{n})} & -k_{1,1}^{(\mathbf{n})} & -k_{0,1}^{(\mathbf{n})} \\ k_{1,0}^{(\mathbf{n})} & 1 & k_{0,1}^{(\mathbf{n})} & -k_{1,1}^{(\mathbf{n})} \\ k_{1,1}^{(\mathbf{n})} & -k_{0,1}^{(\mathbf{n})} & -1 & k_{1,0}^{(\mathbf{n})} \\ -k_{0,1}^{(\mathbf{n})} & -k_{1,1}^{(\mathbf{n})} & -k_{1,0}^{(\mathbf{n})} & -1 \end{bmatrix} \tag{52b}$$

$$\tilde{\mathbf{K}}_{QP_3}^{(\mathbf{n})} = \frac{1}{k^{(\mathbf{n})}} \begin{bmatrix} 1 & -k_{1,0}^{(\mathbf{n})} & -k_{1,1}^{(\mathbf{n})} & -k_{0,1}^{(\mathbf{n})} \\ -k_{1,0}^{(\mathbf{n})} & -1 & -k_{0,1}^{(\mathbf{n})} & -k_{1,1}^{(\mathbf{n})} \\ -k_{1,1}^{(\mathbf{n})} & -k_{0,1}^{(\mathbf{n})} & -1 & k_{1,0}^{(\mathbf{n})} \\ -k_{0,1}^{(\mathbf{n})} & k_{1,1}^{(\mathbf{n})} & -k_{1,0}^{(\mathbf{n})} & -1 \end{bmatrix} \tag{52c}$$

where

$$k^{(\mathbf{n})} = \sqrt{1 + k_{1,0}^{(\mathbf{n})^2} + k_{1,1}^{(\mathbf{n})^2} + k_{0,1}^{(\mathbf{n})^2}} \tag{52d}$$

Since the gain matrices $\tilde{\mathbf{K}}_{QP_1}^{(\mathbf{n})}$, $\tilde{\mathbf{K}}_{QP_2}^{(\mathbf{n})}$, and $\tilde{\mathbf{K}}_{QP_3}^{(\mathbf{n})}$, satisfy the orthogonality requirement in (51), the corresponding 2-D lattice synthesis models are always stable. Hence, there is no need to test the difficult stability conditions in (46) at each stage.

Due to the asymmetric nature of the gain matrices $\tilde{\mathbf{K}}_{HP_1}^{(\mathbf{n})}$ and $\tilde{\mathbf{K}}_{HP_2}^{(\mathbf{n})}$ of the half-plane models in (33) and (44), it is not possible to postulate orthogonal gain matrices. In fact, it requires additional constraints on its parameters to make it stable.

7. Examples and Discussions

In this section, experimental results are obtained from the analysis of several synthetic data sets using the quarter-plane and two asymmetric half-plane models. The proposed parametric estimation theory is tested with the data sets where the autocorrelation functions are exactly known.

In all cases, it was assumed that the autocorrelation function originated from sinusoids buried in white noise, so that the autocorrelation function is of the form

$$r_{yy}(m,n) = \sigma^2\delta(m,n) + \sum_{i=1}^{M} A_i^2 \cos[2\pi(m\mu_i + n\nu_i)] \tag{53}$$

where σ^2 represents the white noise power, M represents the number of sinusoids, A_i^2 represents the power of the i-th sinusoid, and μ_i and ν_i are the frequencies of the i-th sinusoid.

The prediction error filters obtained from the calculated 2-D lattice parameters, factors as discussed in the previous sections. $(\mathbf{n})$-th order power spectrum is determined as follows

$$S_{i,j}^{(\mathbf{n})}(e^{jw_1}, e^{jw_2}) = \frac{1}{\left|B_{i,j}^{(\mathbf{n})}(e^{jw_1}, e^{jw_2})\right|^2} \tag{54}$$

where $(i,j) \in D_{QP}, D_{HP_1}$, or D_{HP_2} which depends upon the method used to compute the 2-D lattice coefficients.

Example 1:

In order to show the effectiveness and the resolution capability of the proposed method, the standard problem of resolving two sinusoids in white noise will be considered. Table 3 shows the parameters used to obtain the autocorrelation function for this example.

Table 3. Parameters of Example 1

M	σ^2	A_i^2	μ_i	ν_i
2	5.0	10.0	0.22	0.10
		10.0	0.20	0.333

In order to determine the most suitable model and the method to be used to compute the lattice parameter factors for this particular example, Table 4 is given. Table 4 shows the calculated third stage minimum mean-square prediction errors with the quarter-plane and the asymmetric half-plane models for all possible ways to obtain the lattice parameters. From Table 4, one can see that the least minimum mean-square prediction error can be obtained by choosing the first asymmetric half-plane model and computing the lattice parameters by minimizing the prediction error field, $e_{1,0}^{(\mathbf{n})}(k_1,k_2)$. The mask of this particular computation is given in Fig. 4(b). Fig. 10 shows the contours of the power spectrum in the spectral domain. It is possible to observe that the first stage model does not resolve any peaks in Fig. 10(a). The second stage model does resolve the two peaks at different locations as shown in Fig. 10(b). Finally, the third stage model completely resolves both peaks at exact locations in Fig. 10(c).

When the minimum mean-square prediction error approaches asymptotically to a certain value, it is found that the power spectrum does not change. In this example, this asymptotic value is $Q_{HP_1}^{(3,3)} = 6.7095994$ which is larger than the variance of the white noise process, i.e., $\sigma^2 = 5.0$ in Table 3.

Table 4. Minimum Mean-Square Prediction Errors of Example 1 for the Third Stage

	$\mathbf{\Lambda}$ = diag.	$Q^{(3,3)}$
	[1 0 0 0]	0.90044282E + 01
	[0 1 0 0]	0.93301529E + 01
Quarter-Plane Model	[0 0 1 0]	0.34004499E + 02
	[0 0 0 1]	0.93774760E + 01
	[1 1 1 1]	0.11636639E + 02
	[1 0 0 0 0]	0.774183350 + 01
	[0 1 0 0 0]	0.67095664E + 01
Model 1	[0 0 1 0 0]	0.11917221E + 02
	[0 0 0 1 0]	0.86667349E + 01
	[0 0 0 0 1]	0.10566658E + 02
	[1 1 1 1 1]	0.14720403E + 02
	[1 0 0 0 0]	0.78074258E + 01
	[0 1 0 0 0]	0.84964503E + 01
Model 2	[0 0 1 0 0]	0.82337289E + 01
	[0 0 0 1 0]	0.70146882E + 01
	[0 0 0 0 1]	0.78970849E + 01
	[1 1 1 1 1]	0.18930582E + 02

However, the determination of the model for any given autocorrelation function still remains to be solved. Initial investigations show that it may be possible to decide how to choose the best model without computing the minimum-prediction error for each stage. Fig. 11 shows the independent autocorrelation points required to determine (**N**)-order lattice parameter factors. It is interesting to note that both asymmetric half-plane models require twice as more autocorrelation points in one direction than the other one. This result is the direct consequence of their mask shown in Fig. 4 and Fig. 6 for Model 1 and Model 2 respectively. If one examines the true locations of the peaks in this example, it will be seen that they are almost parallel to w_2-frequency axis. From Fig. 4(b), it was noted that Model 1 requires more autocorrelation points in n-direction of $r_{yy}(m,n)$. Thus, Model 1 gives the least prediction error and highest resolution of all models. This issue was first discussed by Pendell [30] as directional prediction filters. Further study relating 2-D lattice model determination is currently under investigation.

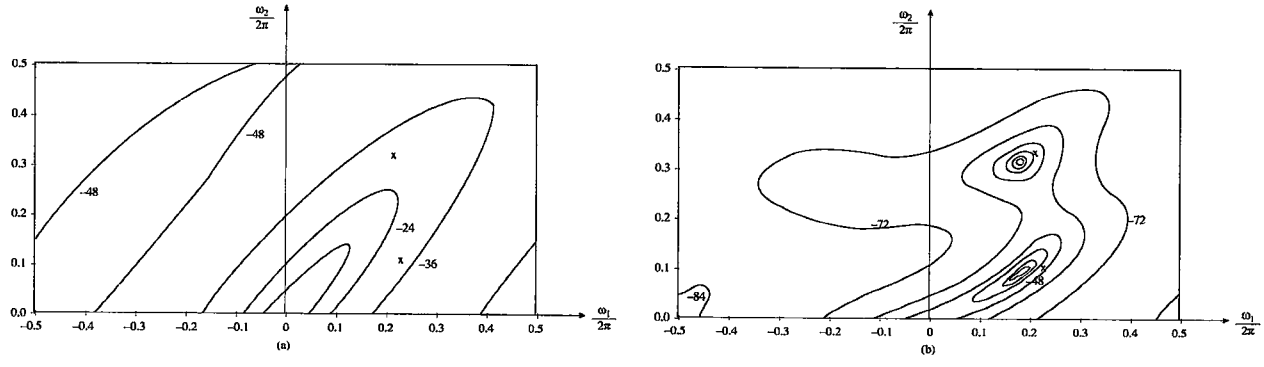

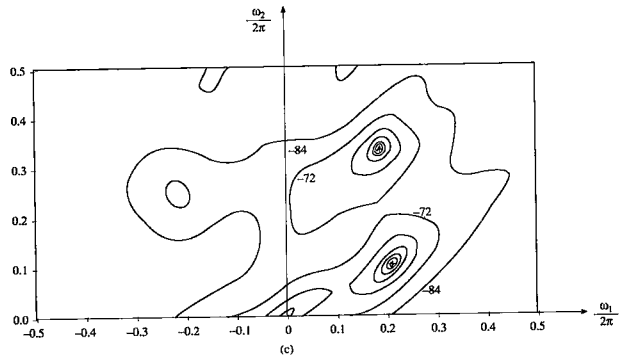

Figure 10. Spectral density contours for example 1; (a) first stage, (b) second stage, (c) third stage.

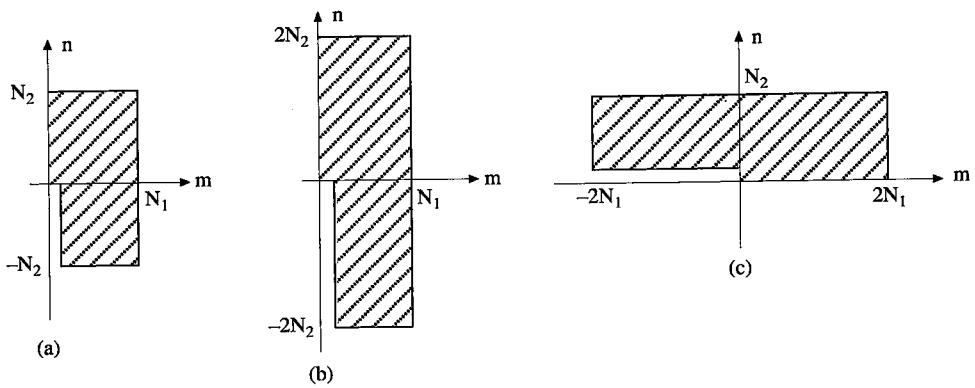

Figure 11. Support domain for the correlation function; (a) quarter-plane, (b) Model 1, (c) Model 2.

Example 2:

In this example, three sinusoids in the white noise are considered. The parameters of the autocorrelation function in (45) are given in Table 5. The third stage minimum mean-square errors of quarter-plane and asymmetric half-plane models are given for all possible values of Λ. From Table 5, it can be seen that the second asymmetric half-plane model gives the smallest minimum mean-square error when the prediction error field, $e_{0,1}^{(\mathbf{n})}(k_1, k_2)$ is minimized, i.e., $\mathbf{\Lambda}_{HP} = \text{diag.matrix}[0\ 0\ 0\ 1\ 0]$.

Table 5. Parameters of Example 2

M	σ^2	A_i^2	μ_i	ν_i
3	0.025	10.0	0.20	0.15
		10.0	0.22	0.25
		10.0	0.32	0.35

Table 6. Minimum Mean-Square Prediction Errors of Example 2 for the Third Stage

	Λ = diag.	$Q^{(3,3)}$
	[1 0 0 0]	0.26482036E + 00
	[0 1 0 0]	0.24030191E + 00
Quarter-Plane Model	[0 0 1 0]	0.12296895E + 02
	[0 0 0 1]	0.25060685E + 00
	[1 1 1 1]	0.13233264E + 00
	[1 0 0 0 0]	0.331594890 + 00
	[0 1 0 0 0]	0.54667306E + 01
Model 1	[0 0 1 0 0]	0.69675462E + 01
	[0 0 0 1 0]	0.83694248E + 01
	[0 0 0 0 1]	0.39316775E + 00
	[1 1 1 1 1]	0.11953115E + 02
	[1 0 0 0 0]	0.36671070E + 00
	[0 1 0 0 0]	0.81138925E - 01
Model 2	[0 0 1 0 0]	0.12571514E + 01
	[0 0 0 1 0]	0.37243524E + 01
	[0 0 0 0 1]	0.40820899E + 00
	[1 1 1 1 1]	0.77485752E + 01

Fig. 12 shows the contours of the spectral density function for successive three stages. The spectral peaks are completely resolved in the third stage as shown in Fig. 12(c). The contours in Fig. 12 constitute a portion of the resolution of the peaks. Fig. 13 shows the half-plane description of the third stage.

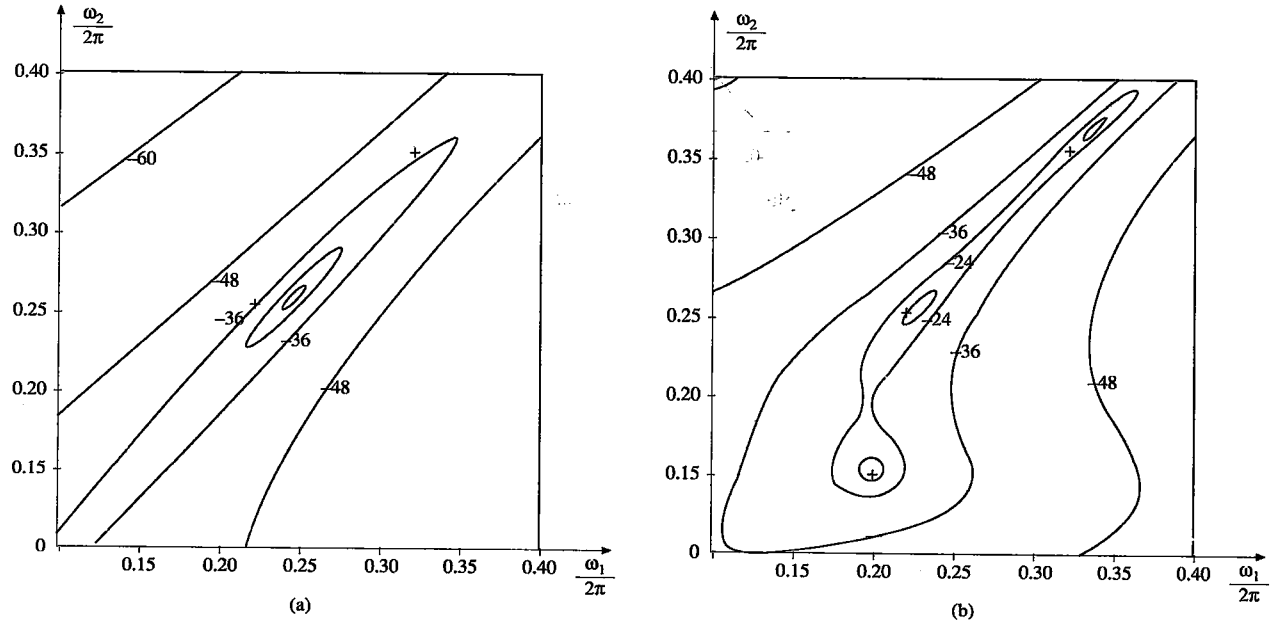

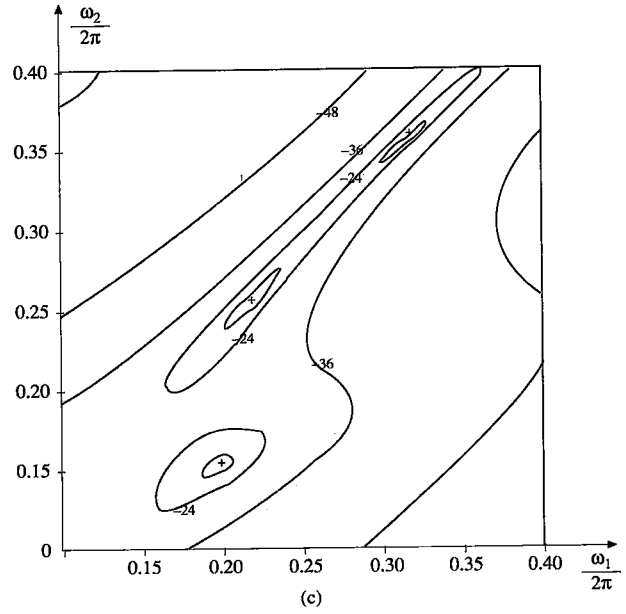

Figure 12. Spectral density contours for example 2: (a) first stage, (b) second stage, (c) third stage.

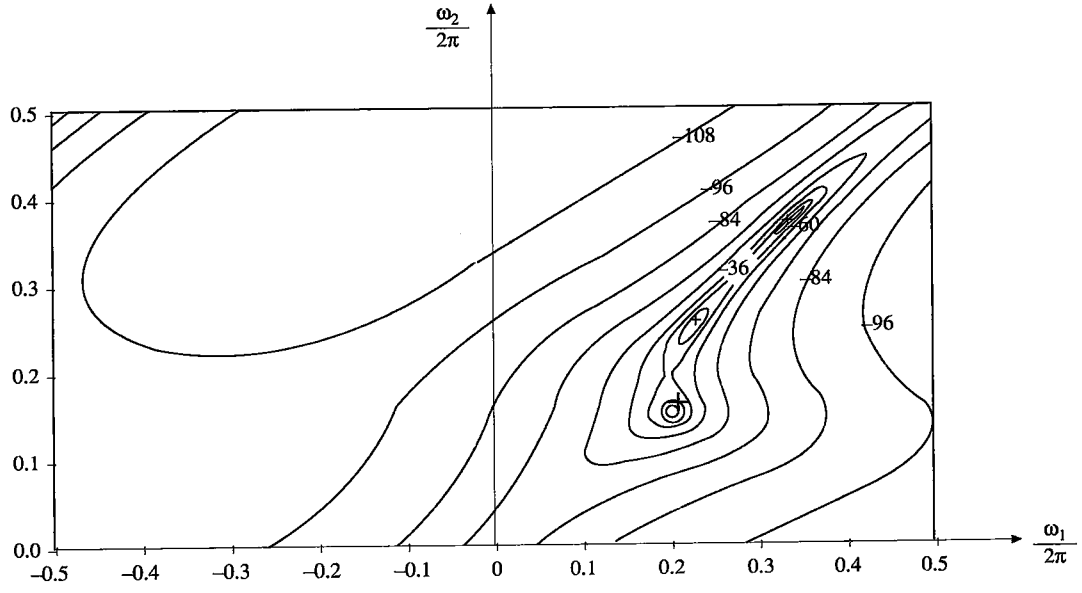

Figure 13. The half-plane description of example 2 for the third stage.

8. Conclusions

In this paper, a parametric 2-D spectral estimation method has been developed. The theory is based upon the appropriate extension of the 1-D lattice theory into 2-D case. It has been shown that it is possible to determine the 2-D spectral estimation of the given autocorrelation function by using lattice parameter factors. Besides being a parametric method, it differs from all other existing methods, in that the order determination problem is eliminated. Examples show high resolution characteristics of the method in the spectral domain.

The author wishes to conclude this paper with the following suggested open research problems:

1) In Sections 3 and 4 only three different lattice models are developed. It is a major concern to investigate all other possible lattice models.

2) The minimum mean-squared prediction error was used as the criteria to determine the best model and the most suitable method to calculate the lattice parameter factors. This approach requires the computation of all the possible cases. However, initial investigations show that it is possible to determine the best model directly from the given autocorrelation function. Hence, it is needed to develop a technique which will enable us to select the model with the minimum error from its autocorrelation function.

3) What is the relationship (if any) between this lattice approach and the maximum entropy method [7]?

REFERENCES

[1] J.W. Woods, "Two-dimensional Markov spectral estimation", IEEE *Trans. Inform. Theory*, Vol.IT-22, pp.552-559, Sept.1976.

[2] J.H. McClellan and R.J. Purdy, "Applications of digital signal processing to radar", in Applications of Digital Signal Processing, A.V. Oppenheim, Ed. Englewood Cliffs, N.J.: Prince-Hall, 1978, pp.239-326.

[3] A.B. Baggeroer, "Sonar signal processing", in Applications of Digital Signal Processing, A.V. Oppenheim, Ed. Englewood Cliffs, N.J.: Prentice-Hall, 1978, pp.331-428.

[4] H.C. Andrews and B.R. Hunt, Digital Image Restoration, Englewood Cliffs, N.J.: Prentice-Hall, 1977, pp.90-112.

[5] J.H. McClellan, "Multidimensional spectral estimation", *Proc. IEEE*, **vol.70**, pp.1029-1039, Sept. 1982.

[6] J. Capon, "High resolution frequency-wavenumber spectrum analysis", *Proc. IEEE*, **vol.57**, pp.1408-1418, Aug.1969.

[7] J.P. Burg, "Maximum entropy spectral analysis", Ph.D. dissertation, Stanford University, Stanford, CA, May 1975.

[8] V.F. Pisarenko, "The retrieval of harmonics from a covariance function", *Geophys. J. Roy. Astron. Soc.*, **vol.33**, pp.347-366, 1973.

[9] P.L. Jackson, L.S. Joyce, and G.B. Feldkamp, "Application of maximum entropy frequency analysis to synthetic aperture radar", in Proc. RADC Spectrum Estimation Workshop (Rome, NY, May 1978), pp.151-157.

[10] O.L. Frost, and T.M. Sullivan, "High resolution two-dimensional spectral analysis", in Proc. ICASSP 79 (Washington, DC, Apr. 1979), pp.673-676.

[11] A.K. Jain, and S. Raganath, "Extrapolation algorithms for discrete signals with application in spectral estimation", *IEEE Trans. Acoust. Speech Signal Proc.*, **vol.ASSP-29**, pp.830-845, Aug. 1981.

[12] L.B. Jackson and H.C. Chien, "Frequency and bearing estimation by two-dimensional linear prediction", in Proc. ICASSP 79 (Washington, DC, April 1979), pp.665-668.

[13] R. Kumaresan, and D.W. Tufts, "A two-dimensional technique for frequency number estimation", *Proc. IEEE*, **vol.69**, pp.1515-1517, Nov. 1981.

[14] A.K. Jain and S. Raganath, "Two-dimensional spectral estimation", in Proc. RADC Spectrum Estimation Workshop (Rome, NY, May 1978), pp.151-157.

[15] J.W. Woods, "Two-dimensional discrete Markovian fields", *IEEE Trans. Inform. Theory*, **vol.IT-18**, pp.232-240, March 1972.

[16] W.I. Newman, "A new method of multi-dimensional power spectral analysis", *Astrm. Astrophys.*, **vol.54**, pp.369-380, 1977.

[17] J.A. Cadzow, and K. Ogino, "Two-dimensional spectral estimation", *IEEE Trans. Acoust., Speech signal Proc.*, **vol.ASSP-29**, pp.396-401, June 1981.

[18] D. Tjostheim, "Autoregressive modelling and spectral analysis of array data in the plane", *IEEE Trans. Geosci. Remote Sensing*, **vol.GE-19**, pp.15-24, Jan. 1981.

[19] S. Roucos, and D.G. Childers, "A two-dimensional maximum entropy spectral estimator", in Proc. ICASSP 79 (Washington, DC, Apr. 1979), pp.669-672.

[20] T.L. Marzetta, "A linear prediction approach to two-dimensional spectral factorization and spectral estimation", Ph.D. dissertation, MIT, Cambridge, MA, Feb. 1979.

[21] T.L. Marzetta, "Two-dimensional linear prediction: Autocorrelation arrays, Minimum-phase prediction error filters, and reflection coefficient arrays", *IEEE Trans. Acoust., Speech, Signal Proc.*, **vol.ASSP-28**, pp.725-733, Dec. 1980.

[22] T.L. Marzetta, "The design of 2-D recursive filters in the 2-D reflection coefficient domain", in Proc. ICASSP 79 (Washington DC, April 1979), pp.665-668.

[23] P. Poehler, and J. Choi, "Linear predictive coding of imagery for data compression applications", in Proc. ICASSP 83 (Boston, MA, April 1983), pp.1240-1243.

[24] J. Makhoul, "Stable and efficient lattice methods for linear predictions", *IEEE Trans. Acoust., Speech, Signal Proc.*, **vol.ASSP-25**, pp.423-428, Oct. 1977.

[25] S.R. Parker and A.H. Kayran, "Lattice parameter autoregressive modelling of two-dimensional fields. Part I - The quarter-plane case", *IEEE Trans. Acount., Speech, Signal Proc.*, **vol.32**, Aug. 1984, pp.872-883.

[26] A.K. Jain, Fundamentals of Digital Image Processing, Englewood Cliffs, N.J.: Prentice-Hall, 1989.

[27] S.R. Parker, and A.H. Kayran, "Lattice parameter autoregressive modelling of two-dimensional fields", Proc. ASSP Spectrum Estimation Workshop (Tampa, FL, November 1983), pp.219-223.

[28] H. Lev-Ari, and S.R. Parker, "Stable and efficient 2-D Lattice Filters", Proc. ICASSP 86 (Tokyo, Japan, April 1986), pp.695-698.

[29] A.H. Gray, Jr., "Passive cascaded lattice digital filters", *IEEE Trans. Circuits Syst.*, **vol.CAS-27**, pp.337-344, May 1980.

[30] J.V. Pendrell, "The maximum entropy principle in two-dimensional spectral analysis", Ph.D. dissertation, York University, Toronto, Ont., Canada, November 1979.

[31] A. Ertuzun, A.H. Kayran, and E. Panayirci, "Stable quarter-plane 2-D lattice filters", Electronics Letters, **vol. 26,** pp. 806-807, June 1990.